https://doi.org/10.5194/egusphere-2026-1236
Preprint. Discussion started: 19 March 2026

Developing tracer interrelationships to derive stratospheric age of air from satellite observations of nitrous oxide

Ariana Elena Castillo[1], Marianna Linz[1,2], Eric Ray[3,4], Laura N. Saunders[5], Kaley A. Walker[5], Gabriele P. Stiller[6], Todd A. Mooring[1], and Stephen Bourguet[1]

[1]Department of Earth and Planetary Sciences, Harvard University, Cambridge, USA
[2]School of Engineering and Applied Sciences, Harvard University, Cambridge, USA
[3]Chemical Sciences Laboratory, Earth Systems Research Laboratory, NOAA, Boulder, USA
[4]Cooperative Institute for Research in Environmental Sciences, University of Colorado Boulder, Boulder, USA
[5]Department of Physics, University of Toronto, Toronto, Canada
[6]Institute of Meteorology and Climate Research, Karlsruhe Institute of Technology, Karlsruhe, Germany

Correspondence to: Ariana Elena Castillo (arianacastillo@fas.harvard.edu)

Abstract. Chemistry-climate models predict a strengthening of the Brewer-Dobson Circulation (BDC) in response to climate change, which has implications for global atmospheric composition, radiation, and climate. This predicted acceleration has not been confirmed with observations, and models also disagree about the mean stratospheric circulation and mixing strength. The BDC impacts the distribution of long-lived tracers and their empirical relationships with one another. Age of air is an important diagnostic for changes in the BDC, and it can be derived from long-lived trace gases, such as sulfur hexafluoride (SF_6) and nitrous oxide (N_2O). We introduce an updated technique to calculate age of air using satellite observations of N_2O. We (1) compute tracer interrelationships of age of air and N_2O (Age:N_2O) and demonstrate that they vary with latitude, and then (2) use these relationships to calculate a new N_2O-derived age timeseries that takes this latitude variability into account from 2005 to 2012. The tracer interrelationships and their variability with latitude provide a better understanding of the structure and seasonality of the BDC. In particular, latitudinally-resolved Age:N_2O relationships reflect the relative importance of photochemical loss of N_2O in different regions and enable hemispheric structural comparisons. The N_2O-age product has more extensive spatial coverage than previous counterparts. Additionally, N_2O and SF_6-age compare well, showing that Age:N_2O relationships are robust on seasonal and interannual time scales. While this timeseries is only 7 years long, this manuscript lays the groundwork for calculating a longer record of N_2O-age to understand long-term variability and shifts of the BDC.

1 Introduction

The Brewer-Dobson Circulation is the large-scale meridional circulation of the stratosphere consisting of upwelling through the tropical tropopause, poleward transport, and downwelling in the midlatitudes and polar regions. The poleward flow consists of two components: a shallow branch and a deep branch (Plumb 2002; Briner and Bönisch 2011). The shallow branch is driven by the breaking of synoptic and planetary-scale waves in the lower stratosphere. Meanwhile, the deep branch is driven by the breaking of planetary waves causing both vertical and horizontal transport in the middle and upper

https://doi.org/10.5194/egusphere-2026-1236
Preprint. Discussion started: 19 March 2026

stratosphere. This large-scale transport plays a pivotal role in atmospheric composition, particularly the distribution of ozone-depleting substances, lifetime of aerosols from wildfires and volcanic eruptions, and water vapor concentrations, all of which have significant impacts on radiation and climate (e.g., Butchart (2014) and references therein).

Climate models predict an acceleration of the BDC in response to a warming climate induced by greenhouse gas increases (Butchart et al., 2010), indicating a projected increase in tropical upwelling at a given pressure height (Butchart et al., 2014). However, observations have not confirmed this increase in circulation strength or acceleration (Engel et al., 2017; Abalos et al., 2021; Garny et al., 2024b; Bourget et al., 2025). One reason is a lack of a long record of stratospheric observations (e.g., via satellite or in situ) that are spatially distributed throughout the Northern and Southern Hemispheres (NH and SH), which would be necessary for a like-to-like comparison of BDC strength between models and observations (Linz et al., 2017; Saunders et al., 2025). To make quantitative conclusions about anthropogenically-forced changes to the circulation strength, a record of stratospheric observations spanning at least 25 years is necessary (Hardiman et al., 2017). Additionally, interannual variations, such as El-Niño Southern Oscillation (ENSO) and the quasi-biennial oscillation (QBO), need to be accounted for when determining trends (Saunders et al., 2025). Studies also suggest that the tropopause – the boundary between the troposphere and stratosphere – is moving upward in response to a warming climate (Oberländer-Hayn et al., 2016). Given the variability and lack of stratospheric observations, there is some ambiguity regarding the extent to which the circulation is truly accelerating versus translating upward.

The magnitude of BDC strength cannot be directly observed; however, it can be inferred from long-lived trace gases, or tracers. Tracers can be measured, and those measurements can be used to calculate circulation strength (e.g., Linz et al., 2016). In addition to real tracers, the idealized tracer, age of air, is a useful metric of stratospheric transport (e.g., Waugh and Hall, 2002; Garny et al., 2024b). Age of air describes how long an air parcel has been in the stratosphere since it entered through the tropical tropopause via upwelling (Hall and Plumb, 1994), thus making age of air an excellent marker of circulation strength. In the context of stratospheric transport, older age indicates slower transit times and younger age indicates faster transit times, incorporating information both about the slow overturning circulation and about the faster quasi-horizontal mixing. Gradients of age can be qualitatively related to both components of the circulation (Linz et al., 2016; Linz et al., 2021) and used to calculate mean circulation strength using observations of long-lived tracers (Linz et al., 2017).

Specifically, the strength of the overturning circulation can be calculated by taking the difference of age between upwelling and downwelling latitudes on a constant potential temperature (θ) contour, or isentrope. This difference between the age of air that is upwelling and downwelling through an isentropic surface is how long it took air to travel from the upwelling region to the downwelling region. Assuming the stratosphere is in steady state and neglecting diabatic diffusion, the age difference is inversely proportional to the strength of the BDC through the same surface:

$$\Delta\Gamma(\theta) = \Gamma_d(\theta) - \Gamma_u(\theta) = \frac{M(\theta)}{\mathcal{M}(\theta)}, \quad (1)$$

https://doi.org/10.5194/egusphere-2026-1236
Preprint. Discussion started: 19 March 2026

where $\Delta\Gamma(\theta)$ is the difference between age through a downwelling ($\Gamma_d(\theta)$) and upwelling ($\Gamma_u(\theta)$) regions on an isentropic surface. M is the mass above the same surface and $\mathcal{M}$ is mass flux through the surface, or the diabatic circulation strength (Linz et al., 2016). In order to evaluate shifts in circulation strength, a long-term record of age is necessary for providing a quantitative measure of the stratospheric circulation.

Age of air cannot be directly observed, but it can be derived from certain long-lived tracers whose concentrations are approximately linearly increasing in the troposphere and are conserved in the stratosphere. As the air traverses the stratosphere, the volume mixing ratio (VMR) acts as a timestamp of when the parcel entered the stratosphere. A tracer is considered conserved when the VMR does not change upon entering the stratosphere due to the lack of chemical sinks. Thus, a tracer that fulfils these criteria is known as a "clock tracer;" both SF_6 and carbon dioxide (CO_2) approximately behave in this way. However, SF_6 has a mesospheric sink from electron capture and photolysis (Morris et al., 1995; Reddmann et al., 2001; Totterdill et al., 2015), and CO_2 is produced by methane oxidation (CH_4) (Wofsy et al., 1972; Andrews et al., 2001) and has a seasonal cycle (e.g., Boering et al., 1996), which complicate calculations of age.

N_2O does not fit these criteria due to photolysis at high altitudes in the stratosphere, but it has a relatively long lifetime estimated at approximately 123 years below 30 km (e.g., SPARC 2013; Fabian et al., 1979; Schmidt et al., 1991; Andrews et al., 2001). However, stratospheric N_2O has been consistently observed with a high spatial and temporal resolution through satellite measurements unlike CO_2, which is not generally retrieved at these altitudes, or SF_6, which has been observed consistently with notable caveats described in Section 2. Regarding N_2O, its higher VMR, compared to that of SF_6, allows for more reliable satellite observations, particularly in the upper stratosphere, such as from Michelson Interferometer for Passive Atmospheric Sounding (MIPAS), Microwave Limb Sounder (MLS), and Atmospheric Chemistry Experiment Fourier Transform Spectrometer (ACE-FTS). Calculating age from N_2O observations would be valuable, as N_2O-derived age (henceforth N_2O-age) would provide extensive spatial and temporal coverage that other satellite-based mean age products, described below, cannot provide.

Since all long-lived tracers are transported by the same circulation, their distributions can provide information about the circulation (Holton, 1986; Mahlman et al., 1986; Plumb, 2007). Given that the distribution of long-lived tracers is impacted by mixing and transport and by chemical sink reactions along their pathway, air 'ages' as it moves both vertically and horizontally. As air is transported upward in the deep tropics, N_2O is gradually exposed to sinks in the upper stratosphere. In the extratropics, newly upwelled air transported from the tropics is mixed with older, downwelled N_2O-depleted air that had been previously exposed to sinks. As a result, age and N_2O (henceforth Age:N_2O) vary with latitude, and thus we expect Age:N_2O to depend on latitude (Plumb, 2007).

Previous studies on Age:N_2O relationships have not considered this latitudinal variability (Andrews et al., 2001; Engel et al., 2002; Strahan et al., 2011). Andrews et al. (2001) mapped CO_2-derived age (CO_2-age) to N_2O concentrations using aircraft and balloon sampled in situ CO_2 and N_2O with a limited meridional and altitude range. Linz et al. (2017) used this single relationship and developed a N_2O-age timeseries from N_2O satellite observations, laying the groundwork for deriving age from an empirical relationship. In addition, previous work calculated age from SF_6 observations, with the first vertically

https://doi.org/10.5194/egusphere-2026-1236
Preprint. Discussion started: 19 March 2026

resolved global age product using SF_6 observations from MIPAS during the 2002-2012 period (Stiller et al., 2008, 2012; Haenel et al., 2015). This spatially and temporally-resolved dataset created a foundation for age of air studies; however, the short time series is only 10 years, which poses a challenge for circulation trend analysis (see Fig. 1 and discussion below). The measurement qualitatively changed after the first few years, making the continuous record even shorter. This limitation motivated more recent work to develop a longer timeseries of global SF_6-derived age (henceforth SF_6-age) with a sink correction applied to MIPAS and ACE-FTS SF_6 described in Section 2 (Saunders et al., 2025; Garny et al., 2024a). Saunders et al. (2025) calculated a new global, satellite-based SF_6-age dataset using ACE-FTS SF_6 observations, including a mesospheric sink correction from Garny et al. (2024a). This dataset spans from February 2004 to February 2021, representing the longest available age of air timeseries from SF_6 profiles. ACE-FTS has much more limited spatial coverage, however, compared to MIPAS. This relative sparsity of ACE-FTS is discussed in more detail in Section 2.2.

This work uses results from these recent studies to introduce a new timeseries of stratospheric age of air derived from N_2O measurements from NASA's MLS and Canadian Spacy Agency's ACE-FTS over the MIPAS time period – 2005-2012. MLS N_2O-age has both the high space-time resolution and temporal coverage that MIPAS and ACE-FTS age products provide separately.

In this study, we present two new data products. (1) We derive latitude-dependent relationships between sink-corrected SF_6-age and N_2O based on MIPAS observations from 2005-2012. We then apply the relationships from (1) to MLS and ACE-FTS N_2O observations to derive a (2) timeseries of N_2O-age from 2005 to 2012. While these timeseries are shorter than previous counterparts, this paper lays the groundwork for an eventual long record of N_2O-age for future long-term variability and trend calculations.

The following section describes the data, and Section 3 covers the methods used in developing the products. In Section 4, the content of both products—MIPAS Age:N_2O and N_2O-derived age from MLS and ACE-FTS will be discussed in detail. Caveats and biases, followed by the reasoning for a shorter timeseries will then be addressed. Finally, we summarize the results and age comparisons.

2 Satellite Datasets

2.1 MIPAS

MIPAS was a Fourier-transform spectrometer launched into a sun-synchronous orbit on Envisat on March 1, 2002. It had a high spatial resolution and a high spectral resolution (5.15-14.6 μm), and it was designed to measure temperature and trace gas abundances, including 20 trace gases (Fischer et al., 2008). Vertical profiles of tracers were measured over an altitude range of 7–70 km on a sun-synchronous orbit, crossing the equator at 10:00 h (morning) and 22:00 h (evening). MIPAS operated at its original full-spectral resolution until March 2004. There was an instrumental issue resulting in a gap from March 2004 to January 2005 before resuming operation, where the spectral resolution decreased from 0.05 cm^{-1} to 0.125 cm^{-1}, although vertical sampling increased by about 20%. After the switch of operation mode in 2004, MIPAS was operated on a

https://doi.org/10.5194/egusphere-2026-1236
Preprint. Discussion started: 19 March 2026

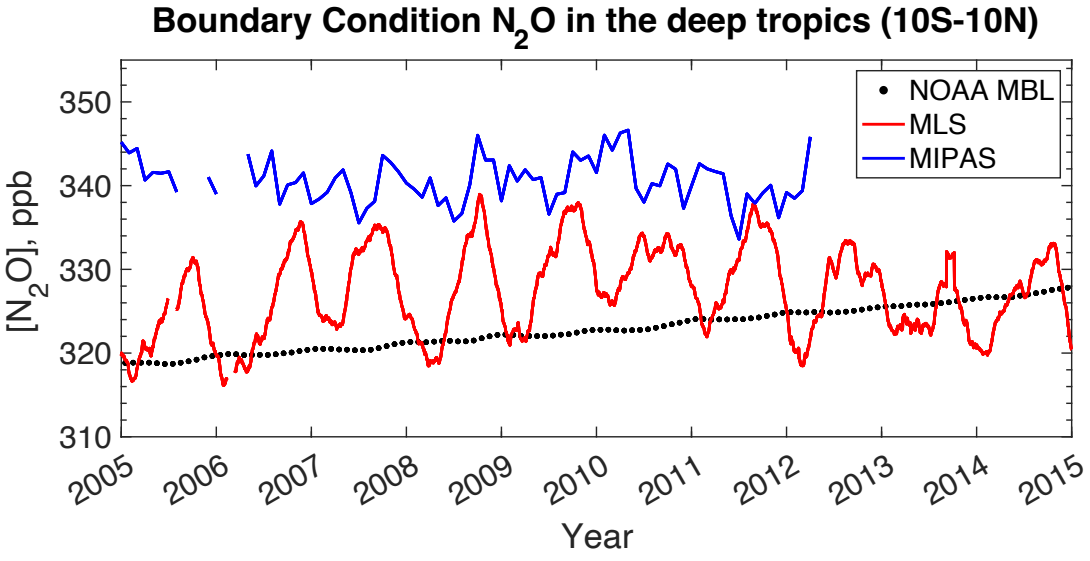

Figure 1: A time series of maximum N_2O concentrations measured by satellites in the deep tropics (10° S-10° N) in the lower stratosphere and tropical NOAA Marine Boundary Layer (MBL) reference N_2O from 2005-2012. Monthly mean N_2O from MIPAS is blue and 14-day running mean MLS v5 N_2O is in red. Data are from NOAA MBL N_2O, MIPAS V5R_224 and V5R_225 N_2O and MLS v5 N_2O.

reduced duty cycle during 2005 and 2006, before it resumed full operation again. Therefore, some gaps in the timeseries during these two years occur. MIPAS collected approximately 1300 individual profiles per day, covering latitudes ranging from 87° S-89° N with an inclination angle of 98.55°. Profile measurements were retrieved on a uniform vertical grid with an altitude range from 6-70 km.

As seen in Fig. 1, the NOAA Marine Boundary Layer (MBL) reference time series demonstrates that the global average N_2O increases in the troposphere. In addition, MBL N_2O (Lan et al., 2026) is plotted to compare with the maximum values observed in the tropics by satellite observations. In this work, we use MIPAS versions V5R_224 and V5R_225 as used in Garny et al. (2024b) (Haenel et al., 2015). SF_6 and N_2O (Plieninger et al., 2015; 2016) retrievals are biased in the deep tropics, with N_2O VMR larger than those from NOAA MBL observations. In contrast to N_2O, SF_6 retrievals are biased lower, thus resulting in older SF_6-age in the tropics compared to that of ACE-FTS SF_6-age and in situ CO_2 and SF_6-age (Garny et al., 2024b, Saunders et al., 2025).

We use SF_6-age of air (with and without a sink correction) created by Saunders et al. (2025) and N_2O to compute a corresponding N_2O product specifically for this study. The monthly zonal mean N_2O and SF_6-age from 2005-2012 on both altitude (km) and θ surfaces were obtained from MIPAS V5R_224 and V5R_225 products. The monthly zonal mean values from the provided dataset are gridded in 5° bins ranging from 90° S to 90° N. In addition, we also evaluate the effects of using SF_6-age with a SF_6 sink correction applied from Garny et al. (2024a) in our analysis.

https://doi.org/10.5194/egusphere-2026-1236
Preprint. Discussion started: 19 March 2026

2.2 ACE-FTS

ACE-FTS is a high-resolution (0.02 cm^{-1}) infrared Fourier-transform spectrometer on SCISAT, a Canadian satellite in a highly inclined orbit that has been taking profile measurements of tracers since February 2004, providing two-decades of consistent satellite observations (Bernath et al., 2005). It is a solar occultation instrument, meaning it collects observations of trace gas concentrations at sunrise and sunset (as seen by the satellite). At each instance, ACE-FTS provides vertical profiles of VMR measurements. The coverage of vertical profiles range from 6 to 150 km (depending on the gas) provided on a 1-km vertical grid. Because it only collects observations at sunrise and sunset – yielding 30 observations a day (2 for each daily orbit) – spatial coverage is limited, particularly in the tropics, and no data exists during Polar night. With an inclination angle of 74°, measurements span up to 85° N and S respectively, and nearly 50% of vertical profile measurements are observed above 60° N and S.

Despite the limited spatial coverage, ACE-FTS is notable for its high signal-to-noise ratio and a wide spectral range (750-4400 cm^{-1}), which enables robust measurements of tracers with small concentrations, including SF_6. Using ACE-FTS for SF_6-age is advantageous, as there are no other datasets that provide consistent SF_6 observations for over 17 years (2004-2021). While there are multiple versions of ACE-FTS, the older versions (v3.5/v3.6 from Feb 2004-Feb 2021) were used for SF_6-age and N_2O for this study because retrievals in recent versions (v4.1/4.2) and most recent version (v5.2) feature unrealistic SF_6 observations between 18–30 km (Boone et al., 2023). The more recent versions have SF_6 observations from Feb 2004 to Present while the older versions v3.5/3.6 only go up to February 2021.

2.3 MLS

MLS (Waters et al., 2006) is a NASA satellite on the Aura mission (Schoeberl et al., 2006), which that was launched on 15 July 2004 and is in a sun-synchronous, near-polar orbit at approximately 705 km with an inclination of 98°. In addition, MLS observes thermal microwave emissions, 190 GHz in the context of N_2O and 18 and 240 GHz for temperature. MLS makes approximately 14 orbits and ~3500 scans per day, to provide daily near-global spatial coverage spanning a latitude range of 82° S to 82° N. This spatial and temporal coverage make MLS unique and particularly useful for our applications. The instrument measures vertical profiles of tracers and chemical constituents. In this study, we use level 2 (swathed), version 5 (v5) of MLS from vertical ranges of 100 hPa to 0.46 hPa, with a vertical resolution of approximately 3km. In particular, we use N_2O (Lambert et al., 2021) and temperature (Schwartz et al., 2021) to calculate θ so both N_2O and N_2O-age are expressed in isentropic coordinates.

Here we use the simplified assumption of the tropical tropopause boundary – the maximum N_2O value at 100hPa between 20° S and 20° N – to address the unphysical seasonality signature from retrievals and to normalize correctly. MLS N_2O increases until around 2010, while after this date, a decrease magnifies over time. This drift becomes apparent in the time series around 2012, but it is not prominently visible in Fig. 1. This drift is height dependent, where it decreases with height (Livesey et al., 2021), and so the drift is not constant with altitude.

https://doi.org/10.5194/egusphere-2026-1236
Preprint. Discussion started: 19 March 2026

In this study, we use MLS N_2O over the same time period as MIPAS (2005-2012) to ensure the most accurate N_2O-derived age that considers both the drift and possible shifts in of SF_6-Age:N_2O relationships that could result in biases in computed N_2O-age over time. We further elaborate on this in Section 3.1

Corrections were applied to account for the drift of decreasing N_2O concentrations in v5 retrievals, but the data still departs from tropospheric observations over time. The seasonal cycle is unrealistically strong in the lowermost tropical stratosphere in v5 MLS, which is not present at all heights and can be seen in Fig. S6. Attempts to account for this spurious seasonal cycle will be discussed in Section 3.1. In addition to the MLS drift and seasonal cycle, both MIPAS and MLS have biased higher N_2O VMR in the tropics (e.g., Fig. 1) that could result in biased younger ages. These biases need to be taken into consideration and will further be addressed in Section 3.1 as well.

Lastly, it is important to make the distinction of MIPAS SF_6-age and N_2O data used to compute Age: N_2O relationships: We used SF_6-age and N_2O on altitude surfaces in Section 3.3.1 and on isentropes in Section 3.3.2.

3 Methodology

The purpose of this work is to derive a record of age that has the high spatial and temporal resolution from N_2O observations by deriving latitude-varying relationships from MIPAS. We derived N_2O-age by using mean SF_6-Age:N_2O relationships from MIPAS (described in Section 3.3.2) to linearly interpolate age using daily MLS v5 N_2O observations from 2005 to 2012 on potential temperature surfaces (θ surfaces) (described in Section 3.4).

3.1 Normalization of N_2O

Satellite observations of N_2O should ideally agree with NOAA MBL observations near the tropical tropopause – the boundary condition of the stratosphere – but they do not. In addition to the biases described in the previous section, it is difficult for limb sounders to accurately observe N_2O in these regions because their vertical resolution is limited resulting from their observation geometry with a long path through all layers of the atmosphere and lowest altitudes are limited due to refraction.

Despite the biases in satellite observed N_2O demonstrated in Fig. 1, it is still possible to use N_2O as a long-lived tracer to develop latitude-dependent Age:N_2O and associated N_2O-age data products. Assuming first order loss, we scale or normalize N_2O to observations in the region where it enters the stratosphere via upwelling, specifically the maximum VMR at each time step. Normalized N_2O, denoted N_2O_{norm}, is a unitless ratio indicating the amount of N_2O remaining since entering the stratosphere via upwelling through the tropical tropopause.

We normalize N_2O using this equation:

$$N_2O_{norm} = \frac{[N_2O]_{obs_{t=n}}}{[N_2O]_{max_{t=n}}}, \quad (2)$$

where the numerator, or $[N_2O]_{obs,t=n}$, is the zonal mean N_2O VMR at the nth time step. The denominator, or $[N_2O]_{max,t=n}$ is the maximum N_2O concentration in the lower stratosphere in the deep tropics or the boundary condition at the corresponding

https://doi.org/10.5194/egusphere-2026-1236
Preprint. Discussion started: 19 March 2026

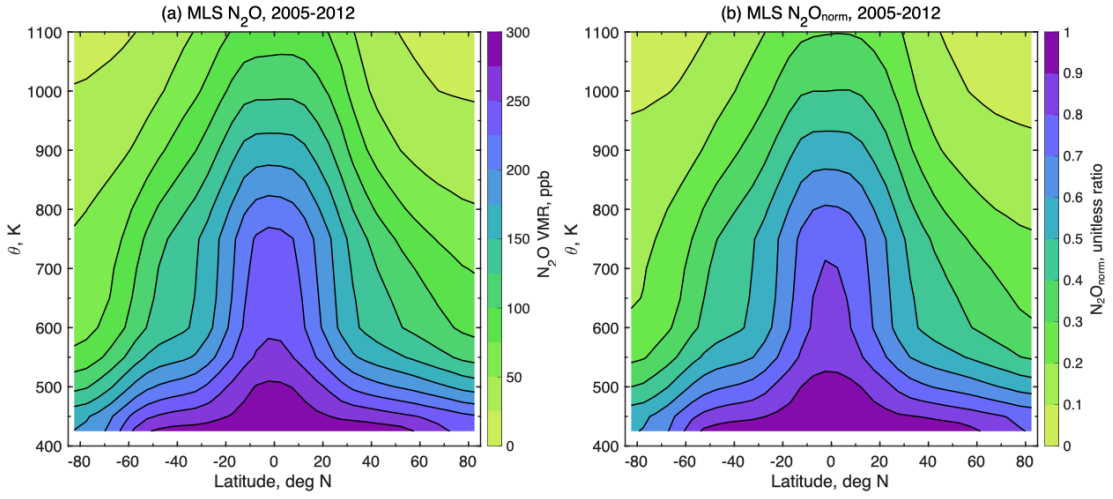

Figure 2: A Mean (a) N_2O concentrations and (b) normalized N_2O as functions of latitude and potential temperature (θ) height coordinate based on MLS v5 N_2O observations from 2005-2012. (a) N_2O concentration contours range from 0 to 300 ppb. (b) Normalized N_2O contours range from 0 to 1in increments of 0.1.

*n*th time step, representing newly upwelled air and thus representing the tropopause value. The deep tropics is defined as 10° S and 10° N for MIPAS, and a larger range of 20° S and 20° N for ACE-FTS due to sparse sampling and 20° S-20° N for MLS (qualitatively the results are the same for 10° S and 10° N). It is important to note that $[N_2O]_{obs,t=n}$ and N_2O_{norm} are space and time dependent. We could have incorporated a time lag such that the denominator would be $[N_2O]_{max,t=n-AoA}$, but this correction is generally quite small (1 ppb/ year, as the trend in N_2O is much smaller than the variations in the stratosphere, and therefore we neglect it here).

Normalizing N_2O makes it easier to compute stable tracer interrelationships over an extended period of time because this transforms observations on to the same scale and takes changing boundary conditions into account. In addition, any bias between instruments is inherently removed during this step in the lower stratosphere, assuming that the bias is constant over altitude and latitude. This is not the case with MIPAS, where the bias is limited to altitudes below ~25km, and MLS, where the impact of the drift decreases with increasing altitude. The biases and variability are demonstrated in Fig. 1, where MLS has a seasonal cycle that is not physically observed in the stratosphere, and this is a signal unique to MLS. In addition, the variability and drift impacts are not constant in time (e.g., Fig. S6), but normalizing to daily maximum values in the deep tropics maps variability on the same scale, although it is not perfect. Nonetheless, normalizing N_2O accounts for the biases of tropical measurements, as seen in Fig. 1, and allows for comparisons using multiple years of observations, thereby enabling the derivation of climatological relationships. The method is also useful because it avoids the limitations of tropopause height – it accounts for the possible shifts in thermal structure over time, potentially allowing for comparisons over multiple decades.

https://doi.org/10.5194/egusphere-2026-1236
Preprint. Discussion started: 19 March 2026

The general shape of the distribution is illustrated in Fig. 2, where we have the zonal mean of MLS v5 N_2O observations as a function of height, or potential temperature (θ), from January 2005 to December 2012. Fig. 2a shows MLS zonal mean VMR, and Fig. 2b shows the zonal mean N_2O_{norm}. In Fig. 2a, the maximum zonal mean N_2O is centered in the deep tropics at θ = 425K, where N_2O abundant air is upwelled into the stratosphere. In this context, the boundary condition is defined as zero age, or Γ = 0 and N_2O_{norm}= 1.0, where air enters the stratosphere. As air moves poleward, it disperses and mixes with air from higher altitudes, that has been subjected to transport through and chemical sinks regions and subsequent photolytic loss of the tracer. Consequently, N_2O_{norm} decreases with latitude and altitude. For example, N_2O_{norm}=1 denotes new or N_2O abundant air (100% remaining), and N_2O_{norm}= 0.02 indicates the air is almost entirely depleted (2% remaining). The shape and distribution of normalized N_2O VMR and N_2O_{norm} is nearly the same, with a bell-shaped structure. Therefore, normalized N_2O also reflects the structure of the stratospheric circulation, making it an excellent scaled metric to better understand the BDC.

3.2 Tracer Interrelationships: Mapping Age of Air with N_2O

3.2.1 Application of tracer interrelationships using satellite observations

Since all tracers are transported by the same circulation, they are all affected by stratospheric transport. Therefore, the distribution of long-lived tracers is primarily determined by transport as well as the chemical or photolytic loss of each tracer (Holton 1986, Mahlman 1986). Because tracer isopleths are closely aligned, if one were to plot one long-lived tracer against the other (henceforth referred to as tracer interrelationships or tracer:tracer relationship, e.g., CH_4:N_2O relationship), this results in compact correlations, meaning that they have a clear mapping with each other (Plumb, 2007). Compactness arises for two reasons: (1) tracers are long-lived, meaning that their stratospheric lifetimes are longer than the timescale of the stratospheric circulation, and (2) tracers are transported by the same circulation (e.g., Fig. 2). The simplest example of tracer interrelationships for two conserved tracers with constant boundary conditions. These 'clock' tracers would scale linearly, so one conserved tracer can be mapped or plotted on to the other with a constant linear slope.

In reality, sinks and boundary conditions vary over time for different tracers. These variables introduce the presence of non-linearities – or curvature – in tracer interrelationships. Fig. 3 demonstrates this, with SF_6-age and N_2O_{norm} plotted against each other. There is a clear non-linear mapping with similar curvature based on satellite observations of MIPAS and ACE-FTS, where mean age increases as N_2O decreases in abundance.

Plumb (2007) demonstrated that tracer relationships also vary meridionally using in situ observations, and we show this in Fig. 3. Mixing between two different regions of the stratosphere can cause spread or variability around the curves at given latitudes. This is because the tropics are relatively isolated from the extratropics (outside of 20° S and 20° N), resulting in a so-called tropical pipe (Neu and Plumb, 1999). This is evident in Fig. 2, where there is a weak vertical gradient above the peak N_2O and θ=550K. Tropical relationships also differ from the extratropics because vertical velocities are smaller than mixing along isentropes, also known as quasi-horizontal mixing. The polar vortex isolates air from the midlatitudes, thus

https://doi.org/10.5194/egusphere-2026-1236
Preprint. Discussion started: 19 March 2026

resulting in different relationships in the higher latitudes. Further discussion on latitude varying tracer interrelationships will be in Section 4.

It is important to note that the 10-degree resolved SF_6-Age:N_2O relationship, as described in Section 3.3.1, is used to discuss tracer interrelationships in the context of latitude-dependence in this section, the sink correction in Section 3.2.2, and hemisphere comparisons in Section 4.1.1.

3.2.2 SF_6 Sink Correction

SF_6 is lost due to a mesospheric sink via electron-capture reactions and photolysis (Morris et al., 1995; Reddmann et al., 2001; Totterrdill et al., 2015). The SF_6-depleted air is rapidly transported downward from the mesosphere into the high latitude stratosphere in the polar vortex each winter, which results in SF_6 depletion at high altitudes and high latitudes (Fisher et al., 1993). When SF_6-age is compared to stratospheric age derived from another long-lived tracer, older SF_6-age is indicative of chemical loss of SF_6 (Ray et al., 2017). Therefore, when the mesospheric sink is not accounted for, the uncorrected SF_6 data result in a bias of towards older ages. This effect can be seen in Fig. 3.

To address biases, more pronounced for older age distributions in the polar regions, we use SF_6-age data provided by Saunders et al. (2025) with a mesospheric sink correction derived by Garny et al. (2024a). The methodologies and detailed descriptions of computing SF_6-age and SF_6-age developing the sink correction are described in both studies respectively.

We provide a brief qualitative summary to provide context for the effects of the SF_6 correction, we refer the interested reader to Saunders et al. (2025) and Garny et al. (2024a) for more detailed descriptions of these methods.

Results of corrected and uncorrected mean SF_6-age as a function of N_2O are displayed in Fig. 3 from MIPAS monthly zonal mean SF_6-age from Saunders et al. (2025). Mean age was calculated by binning age values by latitude, grouping ages that correspond to N_2O_{norm} bins ranging from 0-1 and then calculating mean and standard derivation of each bin. Refer to a more thorough description of computing mean age in Section 3.3.

We show that uncorrected age is older overall in all latitudes, as expected. In addition, the sink-corrected and uncorrected SF_6-age deviations increase with decreasing N_2O and with latitude, also as expected. The inherent impacts of the sink correction on height and latitude are also demonstrated here. Uncorrected SF_6-age increases more with decreasing N_2O than corrected SF_6-age. Meanwhile, the impact of corrected SF_6-age increases with increasing latitude, therefore resulting in a larger age differential at a constant N_2O_{norm} value with increasing latitude, particularly at $N_2O_{norm} \leq 0.7$. In the tropics, particularly at lower N_2O abundances, the difference between corrected and uncorrected SF_6-age is about half a year, compared to the poles where mean SF_6-age is up to 6 years, with error bars reaching 11 years in the upper polar stratosphere, which exceeds the transit time of the BDC (. Thus, SF_6 sink correction impacts increase with both latitude and as N_2O_{norm} decreases.

It is important to note, however, that this sink correction explicitly depends on time and not latitude or altitude. There is an implicit relation to both latitude and altitude because corrected SF_6-age depends on uncorrected SF_6-age, and the uncorrected age varies with both latitude and height. However, this latitude and altitude dependence is not direct, and the influence of the mesosphere is not calculated directly. Because the bias is caused by mesospheric influence, we would expect 2 year-old air

https://doi.org/10.5194/egusphere-2026-1236
Preprint. Discussion started: 19 March 2026

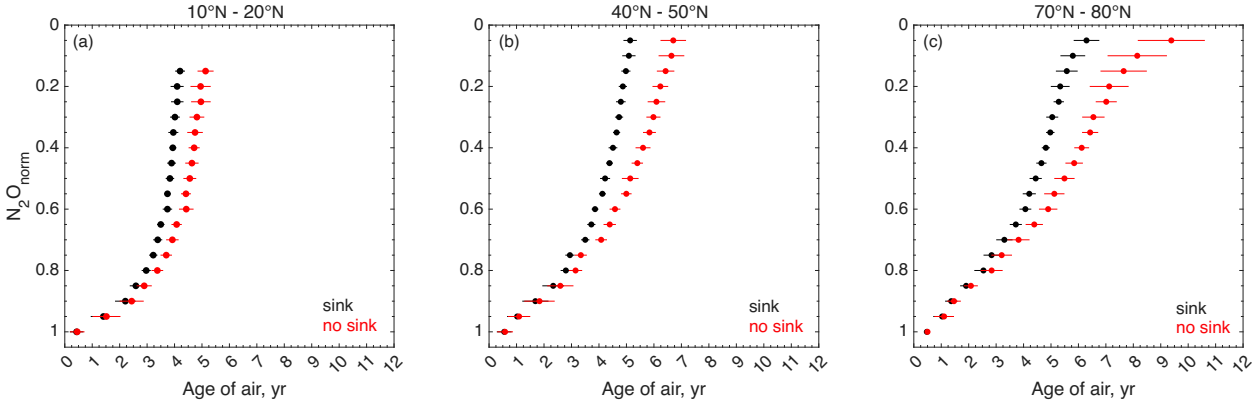

Figure 3: Correlation between normalized N_2O and age of air from original (red) and sink-corrected SF_6 (black) for 3 latitude bands: (a) 10° N-20° N, (b) 40° N-50° N and (c) 70° N-80° N. The solid circles represent the mean age for 0.05 bins of normalized N_2O, with error bars indicating 1 standard deviation. Data are from MIPAS V5R_224 and V5R_225 N_2O and SF_6 observations.

in the tropics to have a different correction than 2 year-old air in the extratropics, for example. Furthermore, the sink correction is solely derived from model data. With limited observations of the stratosphere and mesosphere, there is uncertainty regarding how well the model simulates mesosphere-stratosphere interactions, and hence the sink. Thus, the sink correction cannot completely account for the bias in air older than approximately five years (Garny et al., 2024a).

Nevertheless, the sink correction provides a more accurate depiction of age of air, from satellite measurements in this case, and it also ensures a more accurate mapping of Age:N_2O relationships. As a result, all subsequent uses of the term SF_6-age in this paper refer to an SF_6-derived age with the Garny et al. (2024a) sink correction applied.

3.3 Mapping Mean-Age:N_2O as a function of latitude

This study provides a mapping of Age:N_2O using satellite data spanning both hemispheres. MIPAS SF_6-age and N_2O were used to examine latitudinal relationships in the SF_6-age:N_2O relationship from 2005-2012 because MIPAS sampling is much denser than ACE-FTS (e.g., Fig. 4).

The methodology of deriving SF_6-Age:N_2O relationships is described below. We will describe two Age:N_2O products. In Section 3.3.1, we describe 10-degree resolved relationships as previously described in Section 3.2.1. We want to emphasize that the computed SF_6-Age:N_2O relationship is solely a function of latitude and is fixed in time. In Section 3.3.2, we create a smoothed latitude-varying SF_6-Age:N_2O product to better represent relationships in the deep tropics and extratropics for deriving N_2O -age, which is done in Section 4.2.

3.3.1 Latitude-resolved Mean-Age:N_2O

We derive 18 latitude varying SF_6-Age:N_2O relationships from 36 corresponding 5° latitude bins from 90° S to 90° N. To re-grid SF_6-age and N_2O to a 10° resolution, we take the weighted average of both SF_6-age and N_2O data at a given altitude

https://doi.org/10.5194/egusphere-2026-1236
Preprint. Discussion started: 19 March 2026

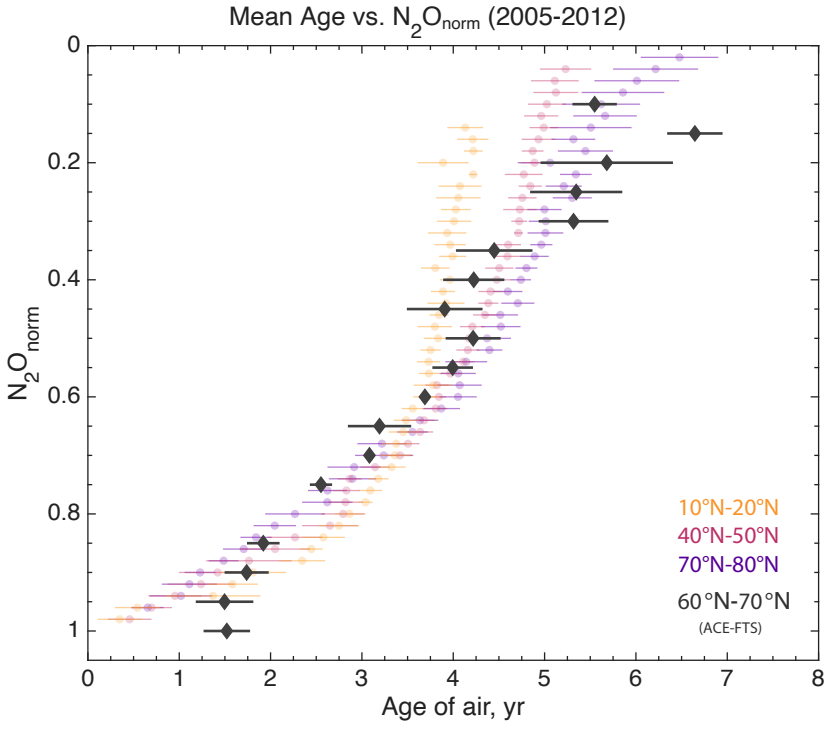

Figure 4: Mean SF_6-age of air versus normalized N_2O at a 10° latitude resolution from 2005-2012. The solid circles represent the mean age for 0.02 bins of normalized N_2O, with error bars indicating 1 standard deviation. Colored points correspond with MIPAS observations. Specific latitude mappings are indicated by dark yellow (10° N-20° N), magenta (40° N-50° N), and purple (70° N-80° N). The diamond points represent the mean age for 0.05 bins of normalized N_2O. The dark grey relationship is derived from ACE-FTS data ranging from 60°-70° latitude. Data are from MIPAS V5R_224 and V5R_225 N_2O and SF_6 observations (multicolor relationships) and ACE-FTS (grey).

ranging from 9.5km to 36.5km. In this case, we average two 5° bins together by weighting the number of respective N_2O and SF_6-age data points within the defined 10° latitude bin sizes.

Mean SF_6-age and standard deviation were calculated by sorting age data in normalized N_2O bins within a N_2O_{norm} range of 0-1. The mean SF_6-age and standard deviation were computed within each respective N_2O_{norm} bin. In this particular example, there are 50 mean age values and the associated standard deviation (+/- σ) representing a range of ages, corresponding to the 50 bins of 0.02 increments of normalized N_2O for each 10° latitude bin, resulting in 18 unique mappings of mean SF_6-Age:N_2O.

The same process was applied to ACE-FTS SF_6-age and N_2O as seen in Fig. 4. The ACE-FTS relationship here reflects the dense sampling poleward of 60°, or in this case, 60° N-70° N. The ACE-FTS relationship agrees overall with MIPAS, but does not capture the curvature observed both with in situ observations (Ray et al., 2024) and MIPAS observations used here. This comparison here shows why MIPAS was selected to compute mappings.

https://doi.org/10.5194/egusphere-2026-1236
Preprint. Discussion started: 19 March 2026

3.3.2 Smoothed Mean-Age:N_2O to derive N_2O-age

In order to create as useful an age product as possible, we create a set of smoothed mean Age:N_2O relationships that accounts for the areas with insufficient observational sampling (see Supplement). This consists of calculating relationships with overlapping bins for a smoother mean SF_6-Age:N_2O product. Refer to S3 for expanded details of binning methods and the resulting Age:N_2O relationships.

3.4 Computing N_2O-derived age of air

MLS v5 N_2O profiles are provided with pressure as the vertical coordinates, so daily θ was calculated separately using temperature profiles corresponding to N_2O observations from 2005 to 2012. Since MLS and MIPAS profiles are not gridded, N_2O and temperature were zonally averaged on the same binned latitude grid as the provided MIPAS and ACE-FTS age products, with values ranging from 90° S to 90° N in 5° bins.

Before interpolating MLS N_2O on the calculated daily θ surfaces, N_2O was normalized with daily maximum N_2O values at 100 hPa between 20° S and 20° N. The rationale for expanding this tropics definition compared to MIPAS and ACE-FTS is due to higher-biased N_2O measurements centered at these extratropical coordinates, where VMR measurements are larger than those at the equator. N_2O_{norm} should be based on the maximum N_2O VMR. Missing values of θ and N_2O were linearly interpolated to realistic values at each latitude and θ bin throughout the timeseries. Subsequently, daily zonal mean N_2O_{norm} was interpolated on θ surfaces ranging from 425K to1100K for each daily time step from 2005 to 2012.

The N_2O-age product is a function of latitude is straightforward: Since tracer interrelationships of SF_6-Age:N_2O from MIPAS and MLS v5 N_2O are now on the same latitude grids, age was linearly interpolated at each 5° latitude grid at each daily time step from 2005-2012. This novel global mapping of mean stratospheric N_2O-age — inferred from satellite data — accounts for horizontal mixing with latitude, and the resulting latitude-varying Age:N_2O relationships.

N_2O-age as a function of time and latitude was also derived using ACE-FTS monthly zonal mean N_2O observations provided by Saunders et al. (2025). The same methodologies as described in this section were used, except that N_2O was normalized with maximum tropical values ranging between 10° S and 10° N, as detailed in Section 3.3.

Results of 1) the latitude-varying SF_6-Age:N_2O, 2) global MLS v5 N_2O-age, and 3) ACE-FTS N_2O-age are provided in Section 4.

4 Results and Discussion

We want to emphasize which data are used in which parts of this study. We use 10° relationships from Section 3.3.1 to discuss tracer interrelationships in Section 4.1. In addition, we use modified, smoothed relationships from Section 3.3.2 for calculating N_2O-age for Sections 4.2, 4.3, and 4.4.

https://doi.org/10.5194/egusphere-2026-1236
Preprint. Discussion started: 19 March 2026

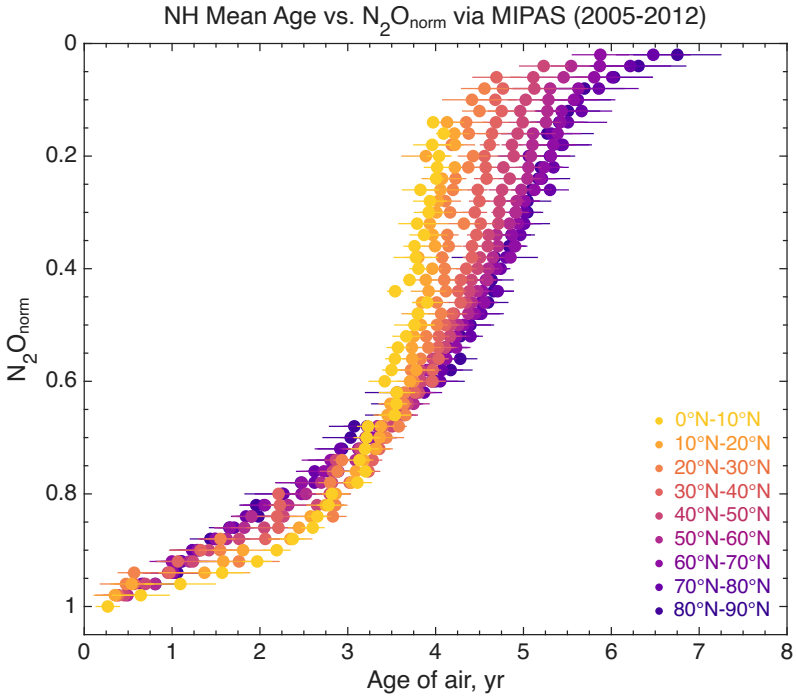

Figure 5: Mean SF_6-age versus normalized N_2O with a latitude resolution of 10° in the NH from 2005-2012. The solid circles represent the mean age for 0.02 bins of normalized N_2O, with error bars indicating 1 standard deviation. Lighter, warmer colors (yellow and orange) represent lower latitudes, while darker, cooler colors (magenta and purple) represent higher latitudes. Data are from MIPAS V5R_224 and V5R_225 N_2O and SF_6 observations.

4.1 Mean-Age:N_2O relationships from MIPAS

We demonstrate that mean-Age:N_2O interrelationships are compact and have a clear meridional dependence (Fig. 5). All mean-Age:N2O relationships indicate that N_2O_{norm} decreases as age of air increases, which is expected. The deep tropics relationship (yellow; 0° N-10° N) is relatively isolated from the extratropics relationships. Notably, the tropical relationship intersects with $\Gamma = 0$ and $N_2O_{norm} = 1$ within uncertainties, aligning with the tropical tropopause boundary condition assumption. We further confirm that relationships are defined by the mixing of younger, recently upwelled air with older, N_2O-depleted air because of subsidence and poleward transport, which results in different Age:N_2O relationships in the extratropics, where subtropics (orange; 10° N-30° N), midlatitudes (magenta; 30° N-60° N) and poles (dark purple; 60° N-90° N) have their own unique mappings.

In addition to insights of stratospheric mixing and transport, the relationships are non-linear, and the presence of curvature is not surprising given N_2O loss throughout the stratosphere. When air enters the stratosphere through the tropopause, it rises gradually and is exposed to N_2O sinks in the middle to upper stratosphere. In the context of tracer interrelationships, air ages with little N_2O loss, and then N_2O_{norm} decreases more rapidly as it ages. Resulting N_2O-depleted air is transported poleward, and this extratropical air ages with minimal exposure to N_2O loss. More specifically, if we assume an isolated tropics with no

https://doi.org/10.5194/egusphere-2026-1236
Preprint. Discussion started: 19 March 2026

mixing, we expect there to be no loss, and so N_2O_{norm} = 1, until air enters the loss region. However, there is some horizontal mixing of extratropical air into the tropics; loss would be slow, and N_2O_{norm} would decrease slowly until air enters the loss region. There is a shift in relationship curvature indicated by notable inflection point, where N_2O_{norm} = 0.7 between ages of 3.0-3.5 years, where N_2O loss begins to dominate in the deep tropics. We demonstrate this via the tropical relationship (yellow) at N_2O_{norm} > 0.7, where N_2O slowly decreases as it ages compared to the extratropical relationships. When air enters the loss region, N_2O decreases rapidly with little aging (from 3.5 to 4 years), and we illustrate this rapid decrease of N_2O starting at N_2O_{norm} < 0.7. Above N_2O_{norm} = 0.7, however, extratropical ages are younger than in the tropics, and so the extratropical relationships are a combination of young, N_2O-abundant air from the tropics and extratropical air that has been exposed to N_2O sinks prior to descent. So extratropics relationships in the lower stratosphere (where N_2O_{norm} > 0.7) act as mixing surfaces between the lower stratosphere tropics and the middle to upper stratosphere. Therefore, we show that the curvature in extratropics relationships are dictated by the N_2O loss, and their meridional variations are a result of transport.

Relationships in SH maintain the same structure and characteristics shown here (refer to Figs. S3 and S4). The SH relationships do have more variability and spread, however. Overall, tracer interrelationships here show that once sinks are considered, as demonstrated here, shifts in relationships can be a useful metric to evaluate perturbations in mixing.

4.1.1 Hemisphere Comparison

We compare NH and SH Age:N_2O interrelationships in Fig.6, which shows relationships in latitude bins via a) 0°-10°; b) 30°-40°; c) 50°-60°; d) 70°-80°. The tropics (Fig. 6a) and poles (Fig. 6d) are roughly symmetric in both hemispheres. This symmetry and compactness are particularly notable in the lower latitudes because results are consistent with an isolated tropics with minimal mixing. At the poles, however, larger standard deviations indicate greater variability in the SH.

Conversely, tracer interrelationships capture stratospheric structure in both hemispheres and demonstrate hemispheric asymmetry in the mixing regions at 30°-40° in Fig. 6b and midlatitudes at 50°-60° in Fig. 6c. This asymmetry is observed in both the mixing region (Fig. 6b) and midlatitudes (Fig. 6c), starting at the inflection point, where N_2O_{norm} = 0.7. Relationships exhibit older mean ages in the SH between N_2O_{norm} 0.7 and 0.3. Results in Fig. 7 demonstrate this as well.

In Fig. 7, we further describe the asymmetric characteristics by taking the absolute differences in mean age in the NH and SH as a function of N_2O_{norm} at 30°-40° (Fig. 7a), 40°-50° (Fig. 7b) and 50°-60° (Fig. 7c). At a constant N_2O_{norm}, SH mean age is older than NH air at almost every N_2O bin between N_2O_{norm} 0.7 and 0.3, with some of the largest departures of just over 0.3 years in Fig. 7a and b and just over 0.4 years in Fig. 7c. It is particularly worth noting that many bins have negative differences larger than the 1σ values.

https://doi.org/10.5194/egusphere-2026-1236
Preprint. Discussion started: 19 March 2026

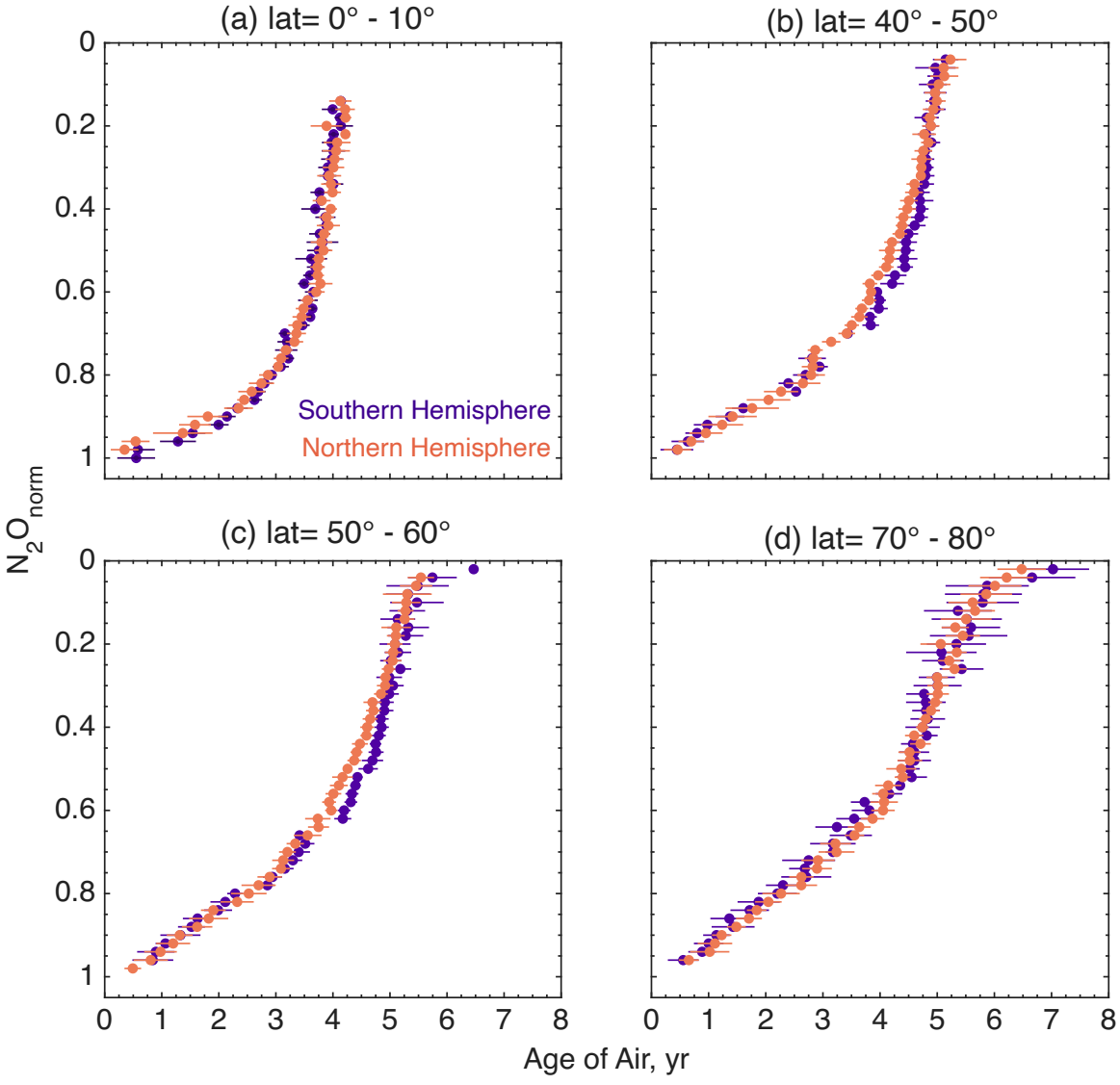

Figure 6: A time series Mean SF_6-age versus normalized N_2O within latitude bins of both hemispheres with (a) Tropics (0-10 degrees), (b) lower midlatitudes (40°-50°), (c) upper midlatitudes (50°-60°) and (d) Polar regions (70°-80°). The solid circles represent the mean age for 0.02 bins of normalized N_2O, with error bars indicating 1 standard deviation. The NH and SH relationships are depicted in purple and orange, respectively. Data are from MIPAS V5R_224 and V5R_225 N_2O and SF_6 observations.

In addition, the opposite mean age differences, that is NH mean age values are older than those in the SH, at higher N_2O_{norm} values, particularly N_2O_{norm} values larger than 0.9. An explanation for this can be described by previous studies focusing on hemisphere asymmetry, particularly linking MLS N_2O anomalies to age shifts. For example, Strahan et al. (2014) found that MLS N_2O anomalies are linked to age variations in the SH midlatitude regions due to the QBO easterly wind phase using

https://doi.org/10.5194/egusphere-2026-1236
Preprint. Discussion started: 19 March 2026

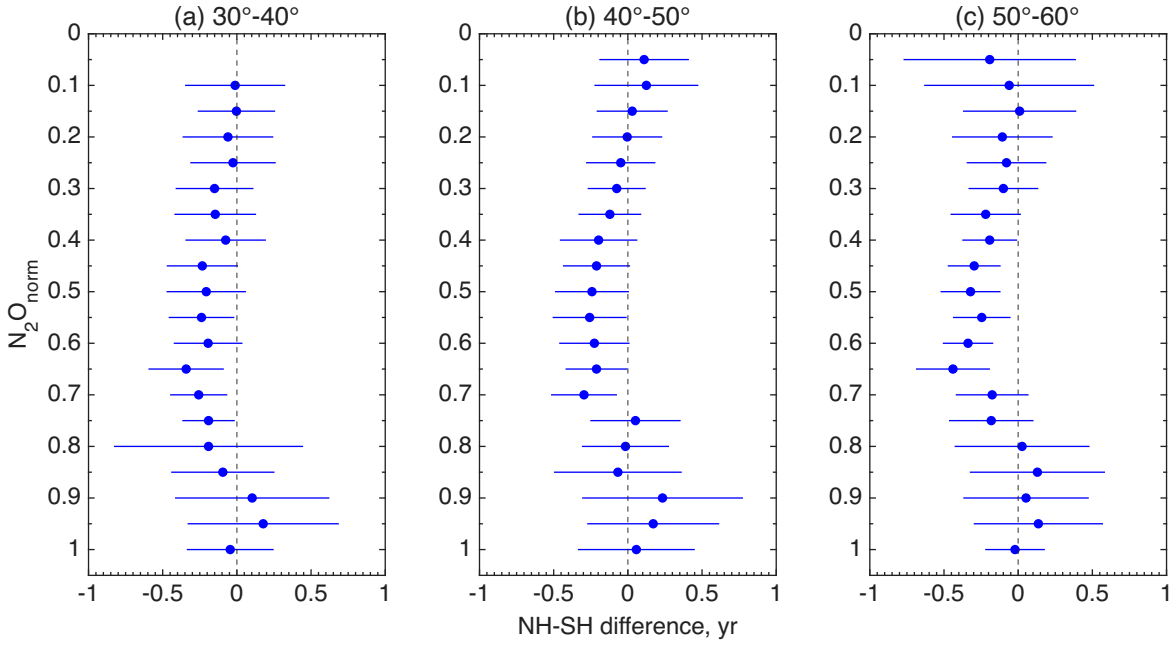

Figure 7: Absolute SF_6-mean age difference between NH and SH (NH – SH) as a function of normalized N_2O in three regions (a) Sub-tropics (20°-30°), (b) Mid-latitudes (40°-50°) and (c) Polar regions (70°-80°). The blue solid circles represent the mean SF_6-age differences for 0.05 bins of normalized N_2O. The error bars are 1 standard deviation, where $\boldsymbol{\sigma_{NH-SH}} = \sqrt{\boldsymbol{\sigma_{NH}^2} + \boldsymbol{\sigma_{SH}^2}}$. Data are from MIPAS v224/225 N_2O and SF_6 observations.

N_2O observations. A follow-up study showed that positive N_2O anomalies, resulting in SH younger ages, coincided with QBO easterly phases during SH winter (Strahan et al., 2015). Both studies use MLS N_2O observations over a comparable time series as our study (2004-2012 for Strahan et al. (2014) and 2005-2012 for Strahan et al., (2015)). Using observations and age of air from reanalyses, Strahan et al. (2020) found that SH extratropical ages have been getting younger by about 0.7 months/decade, significantly driven by stratospheric transport in the SH. We see this signal of younger SH ages in Fig. 7, at N_2O_{norm} > 0.9, and, particularly, in the middle to upper midlatitudes (Fig. 7b and c), where the standard errors are still positive.

While our study does not resolve trends, we observe positive mean age anomalies during the 2005-2012 time period, and SH mean age is younger by a few months at most. It is worth noting, however, that the standard error overlaps with 0 in Fig. 7, consistent with the variability (i.e., Strahan et al., 2020) related to the QBO during this time period. Our study does not remove QBO signals; and given that there were numerous (4) easterly signals during the 2005-2012 time period, the variability in Fig. 7 is consistent with the referenced literature here.

The shapes and curvature of relationships are related to shifting boundary conditions and sinks. We account for the shifting boundary conditions via normalization, which leaves us to account for the photochemical loss of N_2O to provide an explanation for the asymmetry. Since N_2O loss is centered in the upper stratosphere between 30° S and 30° N (SPARC,

https://doi.org/10.5194/egusphere-2026-1236
Preprint. Discussion started: 19 March 2026

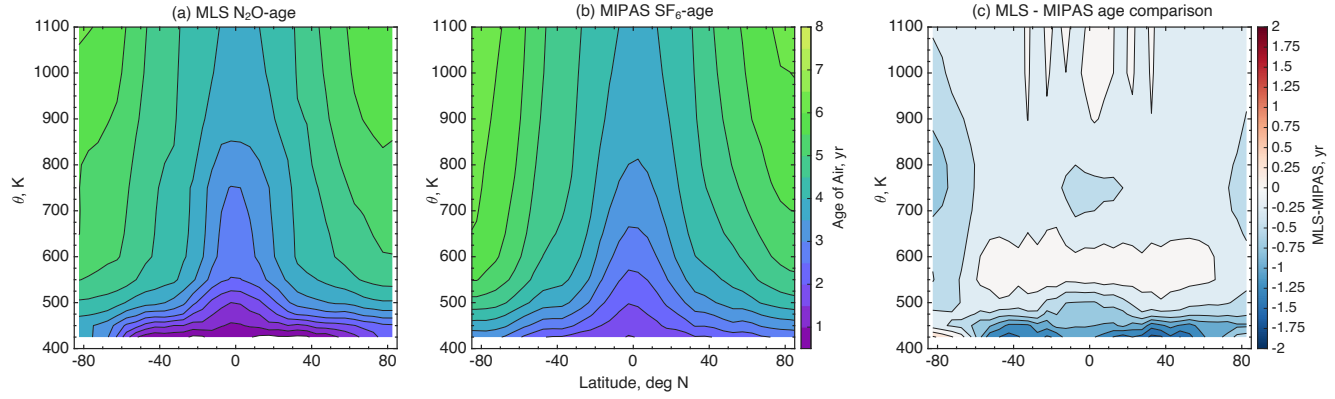

Figure 8: Age as a function of latitude and θ from 2005-2012. (a) N_2O-age computed from MLS N_2O observations via SF_6-Age:N_2O relationships from Fig. 5. (b) SF_6-age from MIPAS. (c) Absolute age difference between MLS N_2O-age (a) and MIPAS SF_6-age (b) (SF_6-age – N_2O-age). (a) and (b) contours are in increments of 0.5 years from 0.5 to 8 years, and (c) contours are in increments of 0.5 years from -2 to 2 years. Data are from MIPAS V5R_224 and V5R_225 N_2O and SF_6 and MLS v5 N_2O observations.

2013), a possible explanation for the asymmetry may be attributed to a difference of transport and mixing in each hemisphere. The BDC has a seasonality, with a stronger circulation in the NH winter that promotes more mixing and overturning of younger air at constant N_2O_{norm} values. With a stronger circulation, N_2O spends less time exposed to N_2O sinks in the tropical upper stratosphere, thus resulting in larger N_2O abundances and inherent younger ages. This explanation is not necessarily surprising, but the precise explanation is unclear, and so we have not specifically detected the contributors here.

4.2 MLS N_2O-age product

We applied the smoothed mean Age:N_2O relationships from Section 3.3.2 to derive mean ages based on MLS v5 N_2O observations from 2005-2012. The results are shown in Fig.8a, which illustrates temporal and zonal mean N_2O-age as a function of latitude and θ. N_2O-age results capture the structure of the BDC. As in Fig. 2, the N_2O-age distribution highlights an isolated tropics, which is characterized by a weak vertical age gradient, indicating minimal horizontal mixing between 20° S-20° N above 550K. With slow vertical velocities and horizontal mixing outside of the tropics, air ages with both increasing height and latitude. More specifically, age isopleths show steeper age contours in the SH, qualitatively suggesting weaker wavebreaking and mixing that drives the circulation average during this time period compared to the NH.

We compare results of MLS N_2O-age (Fig. 8a) with the pre-existing MIPAS SF_6 corrected-age (Fig. 8b) by taking the difference between MLS N_2O-age and MIPAS SF_6-age (Fig. 8c). Much like MLS N_2O-age, MIPAS SF_6-age also shows that age decreases with increasing latitude and confirms the expected zonal mean structure of the stratosphere. It is worth noting, however, the MIPAS SF_6-age is older overall, specifically in the lower stratosphere below 650K and in the polar regions between 700K and 800K, particularly in SH. A possible explanation to the

https://doi.org/10.5194/egusphere-2026-1236
Preprint. Discussion started: 19 March 2026

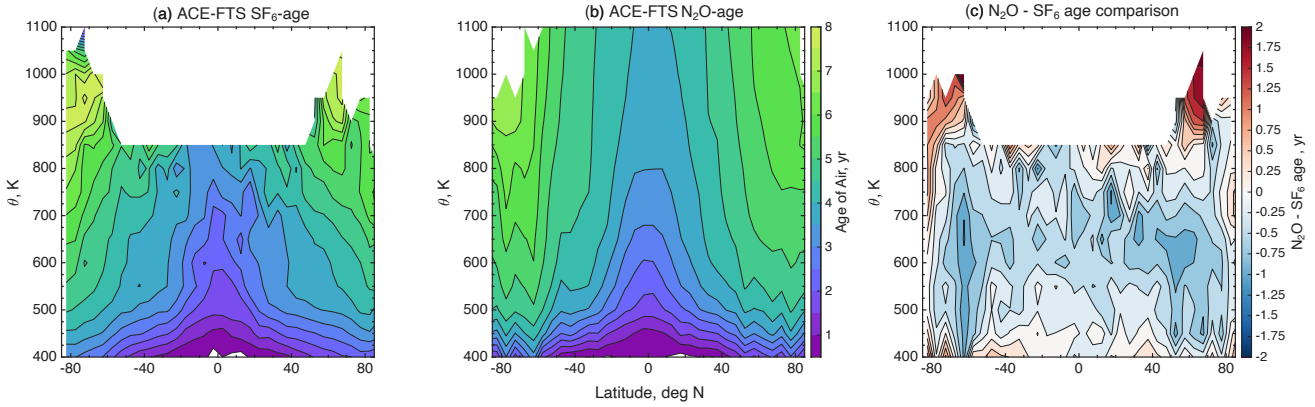

Figure 9: Mean age as a function of latitude and θ from 2005-2012 .(a) SF_6-age from ACE-FTS SF_6 from Saunders et al. (2025). (b) N_2O-age from ACE-FTS N_2O using MIPAS SF_6-Age:N_2O relationships from Fig. 5. (c) Absolute age difference between SF_6-age (a) and N_2O-age (b) (SF_6-age – N_2O-age). (a) and (b) contours are in increments of 0.5 years from 0.5 to 8 years, and (c) contours are in increments of 0.25 years from -2 to 2 years. Data are from ACE-FTS v3.5/3.6 SF_6 and N_2O observations.

older SF_6-age compared to N_2O-age in the SH polar regions is MIPAS' higher bias in the SH polar regions overall, with and without the sink correction (Saunders et al., 2025). For example, the sink corrected MIPAS SF_6-age is just slightly younger than uncorrected ACE-FTS SF_6-age. Compared to MLS N_2O-age, MIPAS SF_6-age is oldest in the mixing regions centered at 40° by up to almost 2 years. This is not surprising given that MIPAS SF_6-age is biased higher in the deep tropics, even with the sink correction applied. Any additional differences in these plots are due to N_2O signatures from MLS and MIPAS observations (i.e., MIPAS N_2O used for SF_6-age:N_2O relationships and MLS N_2O).

4.3 Zonal mean: ACE-FTS Age comparisons

We compare the N_2O-age results with SF_6-age in Fig. 9, which shows zonal mean age for both N_2O-age and SF_6-age from 2005 to 2012. More specifically, Fig. 9a presents zonal mean SF_6-age from ACE-FTS, while Fig. 9b shows the zonal mean N_2O-age computed from ACE-FTS N_2O via MIPAS Age:N_2O relationships. Qualitatively, SF_6-age is characterized by fewer data points and significantly more variability compared to N_2O-age. The discrepancies can be largely attributed to the difficulty of measuring the lower abundances of SF_6, with concentrations at least 5 orders of magnitude less than N_2O. Additionally, the use of latitude-varying Age:N_2O relationships smooths the age isopleths. Albeit there are more bends and kinks in contours compared to that of MLS v5 N_2O-age. Nonetheless, these SF_6 and N_2O-age products confirm the previously inferred structure of the stratospheric circulation.

When we examine the absolute age difference, defined as SF_6-age– N_2O-age, we find that ACE-FTS N_2O-age is generally older throughout most regions, except for the polar upper stratosphere and in the lower stratosphere in the midlatitudes. A possible explanation could be that MIPAS SF_6-age has an old bias relative to ACE-FTS SF_6-age, and MIPAS N_2O has a high bias compared to ACE-FTS N_2O in the lower stratosphere (below ~25 km), most pronounced in the tropics. At a constant ACE-FTS N_2O_{norm}, applying MIPAS relationships would result in older N_2O-age derivations compared to ACE-FTS SF_6-age. In the lower stratosphere, the positive difference between SF_6-age and N_2O-age is notable in mixing regions. There are

https://doi.org/10.5194/egusphere-2026-1236
Preprint. Discussion started: 19 March 2026

positive age departures of up to 2 years in the upper stratosphere in the polar regions where mesospheric air subsides due to the polar vortex. A possible explanation for the large positive age departure in the polar upper stratosphere is the difference of SF_6 abundance compared to N_2O, where SF_6 is approximately 1 ppt or lower while N_2O is approximately 25 ppb, multiple orders of magnitude difference. Since the VMR of SF_6 is so small in the polar upper stratosphere, measurements are not as precise compared N_2O. Another potential reason for the age difference is that the level of SF_6 depletion in descending air is greater than what the Garny et al. (2024a) correction can account for. The oldest age you can derive from the MIPAS SF_6-Age:N_2O relationships is 6.5 years when N_2O_{norm}= 0 (from Fig. 5). The unaccounted for SF_6 loss in the vortex will result in some ACE-FTS mean ages > 6.5 years.

4.4 Timeseries: Age comparisons

A long-term global stratospheric age product provides valuable insights into stratospheric circulation and seasonality. Additionally, a prolonged record of stratospheric age is essential for future long-term variability analysis and circulation trend calculations. While Saunders et al. (2025) derived two SF_6-age products, first from MIPAS (Fig. 10a-b) and second from ACE-FTS spanning 2005 to 2012, we developed an additional more horizontally and temporally resolved N_2O-age product by applying relationships between SF_6-Age:N_2O from MIPAS observations (2005-2012) to MLS N_2O and ACE-FTS N_2O. This study lays the groundwork for an extensive timeseries, and this is ongoing work.

While MIPAS has an age product that has been useful in past studies and provided framework for recently updated products, it fully captures the structure of the stratosphere as seen in Fig. 10a and b. However, it spans only 10 years (taking calibration caveats into consideration reduced that to approximately 7 years), which is not enough for long-term climate trend analysis. ACE-FTS, on the other hand, provides profile observations of stratospheric tracers and a nearly two-decade-long age product. However, the spatial distribution of observations is sporadic, and the low VMR observations of SF_6 result in noisy retrievals and variability. Despite the drift and biased retrievals in the lower stratosphere,

MLS N_2O offers daily profiles over a wide range of latitudes for almost two decades. This provides both invaluable spatial and temporal coverage compared to other satellite products measuring stratospheric tracers.

The results are shown in Fig. 10. This figure displays time series of N_2O-age products from MIPAS, MLS and ACE-FTS satellite observations at θ=450K (Fig. 10a, c, and e) and θ=700K (Fig. 10b, d, and f). The ACE-FTS N_2O-age is represented as the seasonal 3-month average (e.g., JJA, DJF, etc.) mean age over all latitude bins, while the MLS N_2O-age and MIPAS SF_6-age are monthly averages.

All existing age products capture the structure of the BDC, where age is younger in the tropics, older in the midlatitudes, and oldest at the poles. Age also increases with altitude, with younger ages ranging from 0.5 to 2 years in the tropics, as shown in Fig. 10a, c, and e, while Fig. 10b, d and f demonstrate that extratropical ages are older, spanning 2 years onward. This age distribution is consistent with the seasonality of the stratospheric circulation, characterized by upwelling in the tropics and downwelling in poles, particularly in the winter hemisphere at θ levels of 450K and 700K. The impacts of the polar vortex

https://doi.org/10.5194/egusphere-2026-1236
Preprint. Discussion started: 19 March 2026

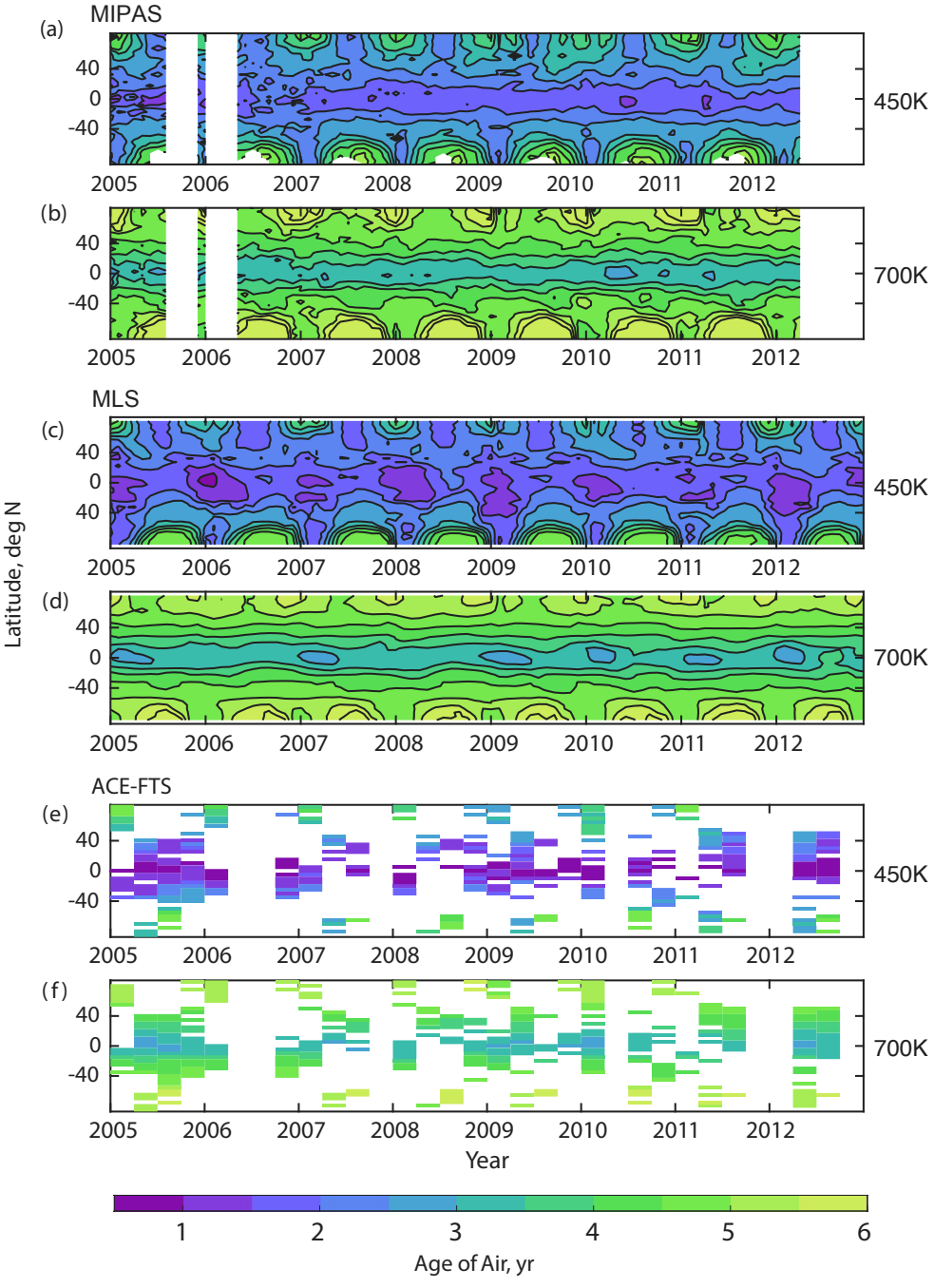

Figure 10: Time series of Age as a function of latitude and θ on constant θ surfaces from 2005 to 2012. (a) Monthly mean MIPAS SF_6-age on θ =450K surface. (b) Monthly mean MIPAS SF_6-age on θ =700K surface. (c) Monthly Mean MLS N_2O-age on θ =450K surface. (d) Monthly Mean MLS N_2O-age on θ= 700K surface. (e) 3-month mean ACE-FTS N2O-age on θ= 450K surface. (f) 3-month mean ACE-FTS N_2O-age on θ= 700K surface. Data of (c) and d) are from MLS v5 N_2O. Data of (e) and (f) are from ACE-FTS v3.5/3.6 observations. Contours are in increments of half a year from 0.5 to 6 years.

https://doi.org/10.5194/egusphere-2026-1236
Preprint. Discussion started: 19 March 2026

are evident during the hemispheric winter, where older air is dispersed when the polar vortex breaks down in late winter and early spring.

Since the time resolution of ACE-FTS N_2O-derived age is significantly coarser than that of the MIPAS and MLS N_2O-age due to lack of consistent spatial coverage, the 3-month N_2O-age product provides a structure of the stratospheric circulation that the SF_6-derived age products have not been able to provide both spatially (compared to ACE-FTS) and temporally (compared to MIPAS). Missing values are prevalent in the higher latitude regions during the wintertime because of absence of sunlight, and therefore the absence of sunrises and sunsets necessary to collect data. However, the points around these 'no sun' signatures reflect the presence of older air at the poles.

The MLS drift begins in 2010 (e.g., Fig. 1). Although a correction has been applied to the MLS N_2O used here (e.g., Livesey et al., 2021) and the drift has been accounted for in in the normalization process, this could introduce a bias of N_2O-age derivations after 2010. For example, a decrease in N_2O values in an environment where its tropospheric abundance is approximately linearly increasing over time, suggests that stratospheric air has experienced greater N_2O loss, hence causing an older bias in the N_2O-age. In addition, the variability of maximum tropical N_2O in below 500K varies by ~40ppb over this time series, which could result in biased age derivations. The θ surfaces are above the 100hPa surface where the drift is most prominent and below the (10hPa) surface with the most variability (as seen in S6), and the age derivations qualitatively agree with MIPAS SF_6-age on both 450K and 700K surfaces.

The results shown in Fig. 10 illustrate the potential of applying latitude-varying Age:N_2O to derive age from N_2O observations. The structure of the MIPAS and ACE-derived age qualitatively agrees with the MLS-derived age. Despite biased MLS N_2O observations, having stratospheric age products from three satellites, is valuable because the addition of the MLS N_2O-age product fills the gaps that ACE-FTS cannot, while MIPAS SF_6-age adds credibility to MLS N_2O-age derivations in this study. The consistency in the spatial structure of both SF_6 and N_2O-age products further demonstrates the effectiveness of normalizing MLS N_2O to address biases and shifting boundary conditions and using latitude-varying Age:N_2O to calculate N_2O-age, thus indicating the robustness of the Age:N_2O product over the 2005-2012 period.

5 Summary

This paper incorporates latitude dependent tracer interrelationships and mean age calculations from long-lived trace gases, which enhances a global perspective of the BDC. When using a midlatitude fixed Age:N_2O relationship to derive N_2O-age at all latitudes (Andrews et al., 2001; Linz et al., 2017), the results will be biased since the latitude dependence would not be included (refer to Fig. S1 in the supplemental). We developed two datasets: (1) tracer interrelationships of SF_6-age vs. N_2O as a function of latitude from MIPAS from 2005-2012 and (2) a N_2O-age of air product derived from MLS and ACE-FTS from 2005-2012. These datasets capture the structure of the BDC in both hemispheres, addressing spatial limitations in stratosphere observations. To account for biased satellite observations in the deep tropics, we normalized N_2O using a defined boundary condition. While the biases are not linear with space and time, we found the normalization is robust when

https://doi.org/10.5194/egusphere-2026-1236
Preprint. Discussion started: 19 March 2026

compared to N_2O observations. A correction was applied to SF_6, and inherently SF_6-age, to account for the mesospheric sink, which reduced mean SF_6-age at lower N_2O_{norm} values and was most profound in the polar regions.

Our analysis revealed a hemisphere symmetrical mean SF_6-Age:N_2O relationships in the deep tropics (10° S-10° N), indicative of an isolated tropics during the study period and in the polar regions (70°-90°). Meanwhile, extratropical (20°-70°) relationships deviated from the tropical and polar relationships at nearly every constant N_2O_{norm} surface. We observed an intersection of all relationships at an inflection point of N_2O_{norm}= 0.7, where N_2O is rapidly lost in the tropics prior to horizontal transport. This inflection point demonstrates that (1) relationships for $N_2O_{norm} > 0.7$ consist of mixing between the outflow of young tropical air and older, N_2O-depleted air from the midlatitudes, and (2) relationships for $N_2O_{norm} < 0.7$ are a result of N_2O photochemistry and horizontal mixing of N_2O depleted air.

Evaluating observations spanning both hemispheres introduced structural differences that have not been previously explored in this way. We found that extratropical (20°-70° N and S) relationships were asymmetric, with NH exhibiting younger mean age values at constant N_2O_{norm} surfaces. SH age is older in the middle atmosphere where $0.3 < N_2O_{norm} < 0.7$, and the departure starts at the inflection point where N_2O_{norm}= 0.7. The asymmetry is possibly attributed to the prevalence of stronger wave-breaking and horizontal mixing in the NH, and thus different rates at which N_2O was lost. Polar regions (70°-90° N and S) are roughly symmetric, with SH relationships exhibiting more variability overall.

We constructed a global mean age product by applying latitude-varying mean SF_6-Age:N_2O relationships to v5 MLS and v3.5/3.6 ACE-FTS N_2O time series from 2005-2012. The dataset showed an expected meridional bell-shaped distribution of mean N_2O-age characterized by youngest age in the lower deep tropics and aging with altitude and latitude, as seen in Fig. 2. Both N_2O-age products illustrate the seasonal dynamics of the circulation. Results of an isolated tropics were confirmed with a small age gradient in the deep tropics, while a stronger horizontal age gradient in the SH exhibited hemisphere asymmetry of the circulation due to less wave-breaking. In addition, MLS N_2O-age captures the spatial and temporal structure of the stratospheric circulation that ACE-FTS SF_6-age does not. Despite the drift in MLS N_2O and non-uniform biases in space and time, mean-age values from ACE-FTS and MIPAS act as a robust confirmation of MLS N_2O-age, which further demonstrates the importance of using normalization as a scaling factor to address the drift.

Comparative analysis of MLS mean N_2O-age and ACE-FTS mean SF_6-age revealed that MLS N_2O-age was younger almost everywhere except for the polar regions where the polar vortex is present, and lower stratosphere in midlatitude regions. The positive age difference in the upper stratosphere at heights greater than 800K suggest a stronger circulation in the upper stratosphere. Comparing MLS N_2O-age with MIPAS SF_6-age showed that MIPAS ages are older almost everywhere, but particularly in the lower stratosphere between 40° S and 40° N and in the polar regions. This comparison not only reveals the biases in MIPAS SF_6-age, aligning with previous studies, but also shows differences are a result of MLS and MIPAS N_2O signatures.

A main takeaway from the comparisons is that the data quality and implementation of latitude-varying stratospheric characteristics lead to different inferred circulation mixing interpretations. We want to reiterate that we do not recommend

https://doi.org/10.5194/egusphere-2026-1236
Preprint. Discussion started: 19 March 2026

using results for trend analysis due to caveats and biases previously stated. Given the biases and limitations in satellite and SF_6 observations, addressing biases and using in situ data will be crucial for future studies. Field campaigns like Dynamics and Chemistry of the of the Summer Stratosphere (DCOTSS) and Stratospheric Aerosol processes, Budget, and Radiative Effects (SABRE) measure long-lived tracers using high-altitude aircraft, but these aircraft only reach altitudes of approximately 21km and are limited to the NH extratropics. Meanwhile, high altitude balloons reach as high as 40 km, and Air-Cores reach heights as far as 30 km, providing robust profiles of stratospheric observations. However, the spatial distribution of AirCores and high-altitude balloons are geographically restricted. To put the lack of spatial and temporal coverage into context, the last time high altitude balloons collected observations in the tropics was in the 1990s. These observations are also predominantly in the NH and turnaround latitudes; having a longer time series of observations spanning both hemispheres would be beneficial as well.

To reduce biases and uncertainties, more comprehensive in situ data spanning multiple decades in both hemispheres are needed. Though, there has been progress to address the biases in N_2O observations while conserving the high spatial resolution of MLS, particularly with the drift and non-physical seasonality signatures. While not available on the duration of this study, a combined N_2O product was created to correct the MLS N_2O drift by using MLS short-term trends and ACE-FTS long-term trends from 2005-2021, part of the Stratospheric Water and OzOne Satellite Homogenized (SWOOSH) package (Davis et al., 2016). We expect younger ages in the lower stratosphere when computing SWOOSH N_2O-age using our SF_6-Age:N_2O product over the 2005-2021 time period. Furthermore, in situ observations have been used to demonstrate that mean-Age:N_2O relationships have shifted from the 1990s to 2020s, where mean age is younger at a constant N_2O_{norm} (Ray et al., 2026). We want to emphasize that our SF_6-Age:N_2O product is fixed in time. Deriving N_2O-ages outside the time period of derivation (2005-2012) is not recommended, as it can introduce biases in age derivations and thus long-term variability and trend inferences by using N_2O -age in this context.

Future work will focus on integrating additional observations to refine latitude-dependent relationships as a function of time and utilizing drift corrected N_2O data for improved age derivations. Addressing the current spatial and temporal gaps will enhance the understanding of long-term stratospheric circulation trends, which impact atmospheric composition and climate.

Data availability

The MIPAS and ACE-FTIS SF_6-age:N_2O products and N_2O-age datasets are available at https://drive.google.com/drive/folders/14Aux1Ww8NYAqQYG9Ulb0s_zYNdmxQHZF?usp=sharing. The age of air datasets from Saunders et al., 2025 are available at https://doi.org/10.5683/SP3/5AC1F0. MLS v5 Level 2 N_2O data can be obtained at https://www.earthdata.nasa.gov/data/catalog/ges-disc-ml2n2o-005. MLS v5 Level 2 temperature data can be obtained at https://www.earthdata.nasa.gov/data/catalog/ges-disc-ml2t-005. The MLS gridded N_2O, pressure, temperature, potential temperature datasets are available at https://drive.google.com/drive/folders/1mGcHVnk5EpzXzmfnVEzqpvGALpC0n-7S?usp=sharing. NOAA N_2O MBL data can be obtained at https://gml.noaa.gov/ccgg/trends_n2o/.

https://doi.org/10.5194/egusphere-2026-1236
Preprint. Discussion started: 19 March 2026

Author contributions

This study was designed by ML and AEC. AEC executed the analysis and wrote the manuscript that built on prior work by LS and ML. LS provided ACE-FTS and MIPAS and developed N_2O datasets for the scope of this study. ML provided expertise in tracer interrelationships, ER provided expertise in in situ observations while KAW and GS provided extensive expertise on the satellite component. TM and SB provided expertise on dynamical transport and stratospheric chemistry respectively. Discussions and valuable feedback were provided by all co-authors throughout this study.

Competing interests

At least one of the (co-)authors is a member of the editorial board of Atmospheric Chemistry and Physics.

Financial support

This project was funded by grants from the NASA New Investigator Program (NIP) Award Number 80NSSC21K0943, NASA Atmospheric Chemistry Modeling and Analysis Program (ACMAP) Award Number 80NSSC23K1005, and NSF CAREER Award Number 2239242.

References

Abalos, M., Calvo, N., Benito-Barca, S., Garny, H., Hardiman, S. C., Lin, P., Andrews, M. B., Butchart, N., Garcia, R., Orbe, C., Saint-Martin, D., Watanabe, S., and Yoshida, K.: The Brewer–Dobson circulation in CMIP6, Atmos. Chem. Phys., 21, 13571–13591, https://doi.org/10.5194/acp-21-13571-2021, 2021.

Andrews, A. E., Boering, K. A., Daube, B. C., Wofsy, S. C., Loewenstein, M., Jost, H., Podolske, J. R., Webster, C. R., Herman, R. L., Scott, D. C., Flesch, G. J., Moyer, E. J., Elkins, J. W., Dutton, G. S., Hurst, D. F., Moore, F. L., Ray, E. A., Romashkin, P. A., and Strahan, S. E.: Mean ages of stratospheric air derived from in situ observations of CO_2 , CH_4 , and N_2 O, J. Geophys. Res., 106, 32295–32314, https://doi.org/10.1029/2001JD000465, 2001.

Bernath, P. F., McElroy, C. T., Abrams, M. C., Boone, C. D., Butler, M., Camy-Peyret, C., Carleer, M., Clerbaux, C., Coheur, P.-F., Colin, R., DeCola, P., DeMazière, M., Drummond, J. R., Dufour, D., Evans, W. F. J., Fast, H., Fussen, D., Gilbert, K., Jennings, D. E., Llewellyn, E. J., Lowe, R. P., Mahieu, E., McConnell, J. C., McHugh, M., McLeod, S. D., Michaud, R., Midwinter, C., Nassar, R., Nichitiu, F., Nowlan, C., Rinsland, C. P., Rochon, Y. J., Rowlands, N., Semeniuk, K., Simon, P., Skelton, R., Sloan, J. J., Soucy, M.-A., Strong, K., Tremblay, P., Turnbull, D., Walker, K. A., Walkty, I., Wardle, D. A., Wehrle, V., Zander, R., and Zou, J.: Atmospheric Chemistry Experiment (ACE): Mission overview, Geophysical Research Letters, 32, https://doi.org/10.1029/2005GL022386, 2005.

https://doi.org/10.5194/egusphere-2026-1236
Preprint. Discussion started: 19 March 2026

Birner, T. and Bönisch, H.: Residual circulation trajectories and transit times into the extratropical lowermost stratosphere, Atmos. Chem. Phys., 11, 817–827, https://doi.org/10.5194/acp-11-817-2011, 2011.

Boering, K. A., Wofsy, S. C., Daube, B. C., Schneider, H. R., Loewenstein, M., Podolske, J. R., and Conway, T. J.: Stratospheric Mean Ages and Transport Rates from Observations of Carbon Dioxide and Nitrous Oxide, Science, 1996.

Boone, C. D., Bernath, P. F., and Lecours, M.: Version 5 retrievals for ACE-FTS and ACE-imagers, Journal of Quantitative Spectroscopy and Radiative Transfer, 310, 108749, https://doi.org/10.1016/j.jqsrt.2023.108749, 2023.

Bourguet, S., Stone, K., and Lickley, M.: Semi-empirical estimates of stratospheric circulation and the lifetimes of chlorofluorocarbons and carbon tetrachloride, Commun Earth Environ, 6, 531, https://doi.org/10.1038/s43247-025-02500-0, 2025.

Butchart, N.: The Brewer-Dobson circulation, Rev. Geophys., 52, 157–184, https://doi.org/10.1002/2013RG000448, 2014.

Butchart, N., Cionni, I., Eyring, V., Shepherd, T. G., Waugh, D. W., Akiyoshi, H., Austin, J., Brühl, C., Chipperfield, M. P., Cordero, E., Dameris, M., Deckert, R., Dhomse, S., Frith, S. M., Garcia, R. R., Gettelman, A., Giorgetta, M. A., Kinnison, D. E., Li, F., Mancini, E., McLandress, C., Pawson, S., Pitari, G., Plummer, D. A., Rozanov, E., Sassi, F., Scinocca, J. F., Shibata, K., Steil, B., and Tian, W.: Chemistry-Climate Model Simulations of Twenty-First Century Stratospheric Climate and Circulation Changes, J. Climate, 23, 5349–5374, https://doi.org/10.1175/2010JCLI3404.1, 2010.

Davis, S. M., Rosenlof, K. H., Hassler, B., Hurst, D. F., Read, W. G., Vömel, H., Selkirk, H., Fujiwara, M., and Damadeo, R.: The Stratospheric Water and Ozone Satellite Homogenized (SWOOSH) database:a long-term database for climate studies, Earth Syst. Sci. Data, 8, 461–490, https://doi.org/10.5194/essd-8-461-2016, 2016.

Engel, A., Strunk, M., Müller, M., Haase, H.-P., Poss, C., Levin, I., and Schmidt, U.: The temporal development of total chlorine in the high latitude stratosphere based on reference distributions of mean age derived from CO2and SF6, J. Geophys. Res., 107, https://doi.org/10.1029/2001JD000584, 2002.

Engel, A., Bönisch, H., Ullrich, M., Sitals, R., Membrive, O., Danis, F., and Crevoisier, C.: Mean age of stratospheric air derived from AirCore observations, Atmospheric Chemistry and Physics, 17, 6825–6838, https://doi.org/10.5194/acp-17-6825-2017, 2017.

Fabian, P., Borchers, R., Weiler, K. H., Schmidt, U., Volz, A., Ehhalt, D. H., Seiler, W., and Müller, F.: Simultaneously measured vertical profiles of H_2 , CH_4 , CO, N_2 O, $CFCl_3$, and CF_2 Cl_2 in the mid-latitude stratosphere and troposphere, J. Geophys. Res., 84, 3149–3154, https://doi.org/10.1029/JC084iC06p03149, 1979.

Fischer, H., Birk, M., Blom, C., Carli, B., Carlotti, M., Clarmann, T. von, Delbouille, L., Dudhia, A., Ehhalt, D., Endemann, M., Flaud, J. M., Gessner, R., Kleinert, A., Koopmann, R., Langen, J., López-Puertas, M., Mosner, P., Nett, H., Oelhaf, H., Perron, G., Remedios, J., Ridolfi, M., Stiller, G., and Zander, R.: MIPAS: an instrument for atmospheric and climate research, Atmos. Chem. Phys., 8, 2151–2188, 2008.

Fisher, M., O'Neill, A., and Sutton, R.: Rapid descent of mesospheric air into the stratospheric polar vortex, Geophysical Research Letters, 20, 1267–1270, https://doi.org/10.1029/93GL01104, 1993.

https://doi.org/10.5194/egusphere-2026-1236
Preprint. Discussion started: 19 March 2026

Garny, H., Eichinger, R., Laube, J. C., Ray, E. A., Stiller, G. P., Bönisch, H., Saunders, L., and Linz, M.: Correction of stratospheric age of air (AoA) derived from sulfur hexafluoride (SF_6) for the effect of chemical sinks, Atmos. Chem. Phys., 24, 4193–4215, https://doi.org/10.5194/acp-24-4193-2024, 2024a.

Garny, H., Ploeger, F., Abalos, M., Bönisch, H., Castillo, A. E., Von Clarmann, T., Diallo, M., Engel, A., Laube, J. C., Linz, M., Neu, J. L., Podglajen, A., Ray, E., Rivoire, L., Saunders, L. N., Stiller, G., Voet, F., Wagenhäuser, T., and Walker, K. A.: Age of Stratospheric Air: Progress on Processes, Observations, and Long-Term Trends, Reviews of Geophysics, 62, e2023RG000832, https://doi.org/10.1029/2023RG000832, 2024b.

Haenel, F. J., Stiller, G. P., von Clarmann, T., Funke, B., Eckert, E., Glatthor, N., Grabowski, U., Kellmann, S., Kiefer, M., Linden, a., and Reddmann, T.: Reassessment of MIPAS age of air trends and variability, Atmospheric Chemistry and Physics Discussions, 15, 14685–14732, https://doi.org/10.5194/acpd-15-14685-2015, 2015a.

Haenel, F. J., Stiller, G. P., Von Clarmann, T., Funke, B., Eckert, E., Glatthor, N., Grabowski, U., Kellmann, S., Kiefer, M., Linden, A., and Reddmann, T.: Reassessment of MIPAS age of air trends and variability, Atmos. Chem. Phys., 15, 13161–13176, https://doi.org/10.5194/acp-15-13161-2015, 2015b.

Hall, T. M. and Plumb, R. A.: Age as a diagnostic of stratospheric transport, J. Geophys. Res., 99, 1059–1070, https://doi.org/10.1029/93JD03192, 1994.

Hardiman, S. C., Lin, P., Scaife, A. A., Dunstone, N. J., and Ren, H.-L.: The influence of dynamical variability on the observed Brewer-Dobson circulation trend, Geophys. Res. Lett., 44, 2885–2892, https://doi.org/10.1002/2017GL072706, 2017.

Holton, J. R.: A dynamically based transport parameterization for one-dimensional photochemical models of the stratosphere, J. Geophys. Res., 91, 2681–2686, https://doi.org/10.1029/JD091iD02p02681, 1986.

Ko, M. K., Newman, P. A., Reimann, S., Strahan, S. E., Atlas, E. L., Burkholder, J. B., Chipperfield, M., Engel, A., Liang, Q., and Plumb, R. A.: Lifetimes of stratospheric ozone-depleting substances, their replacements, and related species, 2013.

Lambert, A.: MLS/Aura Level 2 Nitrous Oxide (N2O) Mixing Ratio V005, https://doi.org/10.5067/AURA/MLS/DATA2515, 2021.

Lan, X., Thoning, K., Dlugokencky, E., and NOAA Global Monitoring Laboratory: Trends in globally-averaged CH4, N2O, and SF6, https://doi.org/10.15138/P8XG-AA10, 2022.

Linz, M., Plumb, R. A., Gerber, E. P., and Sheshadri, A.: The Relationship between Age of Air and the Diabatic Circulation of the Stratosphere, J.. Atmos. Sci., 73, 4507–4518, https://doi.org/10.1175/JAS-D-16-0125.1, 2016.

Linz, M., Plumb, R. A., Gerber, E. P., Haenel, F. J., Stiller, G., Kinnison, D. E., Ming, A., and Neu, J. L.: The strength of the meridional overturning circulation of the stratosphere, Nature Geoscience, 10, 2017.

Linz, M., Plumb, R. A., Gupta, A., and Gerber, E. P.: Stratospheric Adiabatic Mixing Rates Derived From the Vertical Gradient of Age of Air, J. Geophys. Res., 126, e2021JD035199, https://doi.org/10.1029/2021JD035199, 2021.

https://doi.org/10.5194/egusphere-2026-1236
Preprint. Discussion started: 19 March 2026

Livesey, N. J., Read, W. G., Froidevaux, L., Lambert, A., Santee, M. L., Schwartz, M. J., Millán, L. F., Jarnot, R. F., Wagner, P. A., Hurst, D. F., Walker, K. A., Sheese, P. E., and Nedoluha, G. E.: Investigation and amelioration of long-term instrumental drifts in water vapor and nitrous oxide measurements from the Aura Microwave Limb Sounder (MLS) and their implications for studies of variability and trends, Atmos. Chem. Phys., 21, 15409–15430, https://doi.org/10.5194/acp-21-15409-2021, 2021.

Mahlman, J. D., Levy, H., and Moxim, W. J.: Three-dimensional simulations of stratospheric N_2 O: Predictions for other trace constituents, J. Geophys. Res., 91, 2687–2707, https://doi.org/10.1029/JD091iD02p02687, 1986.

Morris, R. A., Viggiano, A. A., Arnold, S. T., and Paulson, J. F.: Chemistry of atmospheric ions reacting with fully fluorinated compounds, International Journal of Mass Spectrometry and Ion Processes, 149–150, 287–298, https://doi.org/10.1016/0168-1176(95)04258-M, 1995.

Neu, J. L. and Plumb, R. A.: Age of air in a “leaky pipe” model of stratospheric transport, J. Geophys. Res., 104, 19243–19255, https://doi.org/10.1029/1999JD900251, 1999.

Oberländer-Hayn, S., Gerber, E. P., Abalichin, J., Akiyoshi, H., Kerschbaumer, A., Kubin, A., Kunze, M., Langematz, U., Meul, S., Michou, M., Morgenstern, O., and Oman, L. D.: Is the Brewer–Dobson circulation increasing or moving upward?, Geophys. Res. Lett., 43, 1772–1779, https://doi.org/10.1002/2015GL067545, 2016.

Plieninger, J., Clarmann, T. von, Stiller, G. P., Grabowski, U., Glatthor, N., Kellmann, S., Linden, A., Haenel, F., Kiefer, M., Höpfner, M., Laeng, A., and Lossow, S.: Methane and nitrous oxide retrievals from MIPAS-ENVISAT, Atmos. Meas. Tech., 8, 4657–4670, https://doi.org/10.5194/amt-8-4657-2015, 2015.

Plieninger, J., Laeng, A., Lossow, S., Clarmann, T. von, Stiller, G. P., Kellmann, S., Linden, A., Kiefer, M., Walker, K. A., Noël, S., Hervig, M., McHugh, M., Lambert, A., Urban, J., Elkins, J. W., and Murtagh, D.: Validation of revised methane and nitrous oxide profiles from MIPAS-ENVISAT, Atmos. Meas. Tech., 9, 765–779, https://doi.org/10.5194/amt-9-765-2016, 2016.

Plumb, R. A.: Stratospheric Transport, J. Meteor. Soc. Japan, 80, 793–809, https://doi.org/10.2151/jmsj.80.793, 2002.

Plumb, R. A.: Tracer interrelationships in the stratosphere, Rev. Geophys., 45, 1–33, https://doi.org/10.1029/2005RG000179, 2007.

Rao, J., Yu, Y., Guo, D., Shi, C., Chen, D., Hu, D., ,Key Laboratory of Meteorological Disaster, Ministry of Education (KLME)/Joint International Research Laboratory of Climate and Environment Change (ILCEC)/Collaborative Innovation Center on Forecast and Evaluation of Meteorological Disasters (CIC-FEMD), Nanjing University of Information Science & Technology, Nanjing 210044, China, ,State Key Laboratory of Numerical Modeling for Atmospheric Sciences and Geophysical Fluid Dynamics, Institute of Atmospheric Physics, Chinese Academy of Sciences, Beijing 100029, China, and ,Fredy & Nadine Herrmann Institute of Earth Sciences, The Hebrew University of Jerusalem, Edmond J. Safra Campus, Givat Ram Jerusalem 91904, Israel: Evaluating the Brewer–Dobson circulation and its responses to ENSO, QBO, and the solar cycle in different reanalyses, Earth and Planetary Physics, 3, 1–16, https://doi.org/10.26464/epp2019012, 2019.

https://doi.org/10.5194/egusphere-2026-1236
Preprint. Discussion started: 19 March 2026

Ray, E. A., Moore, F. L., Elkins, J. W., Rosenlof, K. H., Laube, J. C., Röckmann, T., Marsh, D. R., and Andrews, A. E.: Quantification of the SF_6 lifetime based on mesospheric loss measured in the stratospheric polar vortex, J. Geophys. Res.: Atmos., https://doi.org/10.1002/2016JD026198, 2017.

Ray, E. A., Moore, F. L., Garny, H., Hintsa, E. J., Hall, B. D., Dutton, G. S., Nance, D., Elkins, J. W., Wofsy, S. C., Pittman, J., Daube, B., Baier, B. C., Li, J., and Sweeney, C.: Age of air from in situ trace gas measurements: insights from a new technique, Atmos. Chem. Phys., 24, 12425–12445, https://doi.org/10.5194/acp-24-12425-2024, 2024.

Reddmann, T., Ruhnke, R., and Kouker, W.: Three-dimensional model simulations of SF6 with mesospheric chemistry, J. Geophys. Res., 106(D13), 14525–14537, https://doi.org/doi:10.1029/2000JD900700, 2001.

Saunders, L. N., Walker, K. A., Stiller, G. P., Von Clarmann, T., Haenel, F., Garny, H., Bönisch, H., Boone, C. D., Castillo, A. E., Engel, A., Laube, J. C., Linz, M., Ploeger, F., Plummer, D. A., Ray, E. A., and Sheese, P. E.: Age of air from ACE-FTS measurements of sulfur hexafluoride, Atmos. Chem. Phys., 25, 4185–4209, https://doi.org/10.5194/acp-25-4185-2025, 2025.

Schmidt, U., Bauer, R., Khedim, A., Klein, E., Kulessa, G., and Schiller, C.: Profile observations of long-lived trace gases in the Arctic vortex, Geophys. Res. Lett., 4, 767–770, https://doi.org/10.1029/91GL00552, 1991.

Schoeberl, M. R., Douglass, A. R., Hilsenrath, E., Bhartia, P. K., Beer, R., Waters, J. W., Gunson, M. R., Froidevaux, L., Gille, J. C., Barnett, J. J., Levelt, P. F., and DeCola, P.: Overview of the EOS aura mission, IEEE Trans. Geosci. Remote Sensing, 44, 1066–1074, https://doi.org/10.1109/TGRS.2005.861950, 2006.

Schwartz, M.: MLS/Aura Level 2 Temperature V005, https://doi.org/10.5067/AURA/MLS/DATA2520, 2021.

Stiller, G. P., Clarmann, T. v, Höpfner, M., Glatthor, N., Grabowski, U., Kellmann, S., Kleinert, A., Linden, A., Milz, M., Reddmann, T., Steck, T., Fischer, H., Funke, B., López-Puertas, M., and Engel, A.: Global distribution of mean age of stratospheric air from MIPAS SF_6 measurements, Atmos. Chem. Phys., 8, 677–695, 2008.

Stiller, G. P., von Clarmann, T., Haenel, F., Funke, B., Glatthor, N., Grabowski, U., Kellmann, S., Kiefer, M., Linden, a., Lossow, S., and López-Puertas, M.: Observed temporal evolution of global mean age of stratospheric air for the 2002 to 2010 period, Atmos. Chem. Phys., 12, 3311–3331, https://doi.org/10.5194/acp-12-3311-2012, 2012.

Strahan, S. E., Douglass, A. R., R. S. Stolarski, H. Akiyoshi, S. Bekki, P. Braesicke, N. Butchart, M. P. Chipperfield, D. Cugnet, S. Dhomse, S. M. Frith, A. Gettelman, S. C. Hardiman, D. E. Kinnison, J.F. Lamarque, E. Mancini, M. Marchand, M. Michou, O. Morgenstern, T. Nakamura, and Olivie, D.: Using transport diagnostics to understand chemistry climate model ozone simulations, J. Geophys. Res., 116, https://doi.org/10.1029/2010JD015360, 2011.

Strahan, S. E., Douglass, A. R., Newman, P. A., and Steenrod, S. D.: Inorganic chlorine variability in the Antarctic vortex and implications for ozone recovery, JGR Atmospheres, 119, https://doi.org/10.1002/2014JD022295, 2014.

Strahan, S. E., Oman, L. D., Douglass, A. R., and Coy, L.: Modulation of Antarctic vortex composition by the quasi-biennial oscillation, Geophysical Research Letters, 42, 4216–4223, https://doi.org/10.1002/2015GL063759, 2015.

Strahan, S. E., Smale, D., Douglass, A. R., Blumenstock, T., Hannigan, J. W., Hase, F., Jones, N. B., Mahieu, E., Notholt, J., Oman, L. D., Ortega, I., Palm, M., Prignon, M., Robinson, J., Schneider, M., Sussmann, R., and Velazco, V. A.:

https://doi.org/10.5194/egusphere-2026-1236
Preprint. Discussion started: 19 March 2026

Observed Hemispheric Asymmetry in Stratospheric Transport Trends From 1994 to 2018, Geophys. Res. Lett., 47, e2020GL088567, https://doi.org/10.1029/2020GL088567, 2020.

Totterdill, A., Kovacs, T., Gomez Martin, J. C., Feng, W., and Plane, J. M. C.: Mesospheric Removal of Very Long-Lived Greenhouse Gases SF6 and CFC-115 by Metal Reactions, Lyman-α Photolysis, and Electron Attachment, J. Phys. Chem. A, 119, 2016–2025, https://doi.org/10.1021/jp5123344, 2015.

Waters, J. W., Froidevaux, L., Harwood, R. S., Jarnot, R. F., Pickett, H. M., Read, W. G., Siegel, P. H., Cofield, R. E., Filipiak, M. J., Flower, D. A., Holden, J. R., Lau, G. K., Livesey, N. J., Manney, G. L., Pumphrey, H. C., Santee, M. L., Wu, D. L., Cuddy, D. T., Lay, R. R., Loo, M. S., Perun, V. S., Schwartz, M. J., Stek, P. C., Thurstans, R. P., Boyles, M. A., Chandra, K. M., Chavez, M. C., Gun-Shing Chen, Chudasama, B. V., Dodge, R., Fuller, R. A., Girard, M. A., Jiang, J. H., Yibo Jiang, Knosp, B. W., LaBelle, R. C., Lam, J. C., Lee, K. A., Miller, D., Oswald, J. E., Patel, N. C., Pukala, D. M., Quintero, O., Scaff, D. M., Van Snyder, W., Tope, M. C., Wagner, P. A., and Walch, M. J.: The Earth observing system microwave limb sounder (EOS MLS) on the aura Satellite, IEEE Trans. Geosci. Remote Sensing, 44, 1075–1092, https://doi.org/10.1109/TGRS.2006.873771, 2006.

Waugh, D. and Hall, T. M.: Age of stratospheric air: Theory, observations, and models, Rev. Geophys., 40, 1010, https://doi.org/10.1029/2000RG000101, 2002.

Wofsy, S. C., McConnell, J. C., and McElroy, M. B.: Atmospheric CH_4 , CO, and CO_2, J. Geophys. Res., 77, 4477–4493, https://doi.org/10.1029/JC077i024p04477, 1972.